

# Interfaces in Polycrystals

## CHAPTER PREVIEW

This chapter is part 2 of the three-part series on interfaces. Crystalline solids usually consist of a large number of randomly oriented grains separated by grain boundaries (GBs). Each grain is a single crystal and contains many of the defects already described.

A GB is defined as the surface between any two grains that have the same crystal structure and composition.

Many GBs, but not all, can be modeled as arrays of dislocations.

The dislocation model can be misleading; the GBs that may be most important in a ceramic may be the ones that do not appear to contain dislocations. So the warning is, we may sometimes concentrate on a particular type of GB just because we can understand that type of GB. Unless we fully understand GBs in ceramics, we will never have a full understanding of what happens during ceramic processing or why ceramics have certain mechanical properties, conductivity (thermal or electrical), etc. GBs become even more important as fine-grained nanostructured ceramics become more available. We also need to understand the junctions formed when three or four grains join: these are known as triple junctions (TJs) and quadruple junctions (QJs), which we might regard as new line and point defects, respectively. We conclude with a discussion of properties, not because they are unimportant (nor because of the bias of the authors). We want to understand GBs so as to explain some properties and to predict others.

## 14.1 WHAT ARE GRAIN BOUNDARIES?

Grain boundaries are internal interfaces and behave much like external surfaces, but now we have to be concerned with two crystal orientations, not one. Just as for surfaces, we have a pressure difference associated with the GB curvature and a driving force that tends to lead to an overall increase in grain size whenever possible. Grain morphology and GB topology are two aspects of the same topic. It is instructive to think of the model of soap foams: a soap film is flat when in equilibrium and it has a finite thickness. Three soap films meet along a line—a TJ. If you blow on a soap film (apply a pressure) it bows out until the “surface tension” balances the applied pressure.

Whenever we join two grains of the same composition and structure, we form a GB. The grains are related to one another by a

rotation axis and meet on a plane, which may be curved. The rotation axis is fixed only for a given boundary and is not unique, even for that boundary; there are different ways to form the same GB. We start by considering two identical grains. Fix one grain and rotate the other about any axis. Cut each crystal parallel to a particular flat plane (to keep it simple) in space and join the grains at this plane. This plane is the GB. Then allow the atoms to relax to a low-energy configuration (which may not be the minimum energy).

The conventional approach is to consider four types of GB based on the symmetry operation used to create them:

twist, tilt, mixed, and twin.

The first two (and hence the third) designations are really helpful only when the misorientation angle is small (low-angle GBs). This description is based on the location of the rotation axis.

### TWIST, TILT, TWIN, LOW, HIGH, AND “GENERAL”

Twist	$n$ normal to plane
Tilt	$n$ parallel to plane
Twin boundary	Mirror across GB plane
Low-angle GB	$\theta < 10^\circ$ (low is small!)
High-angle GB	Structured, $\theta > 10^\circ$
General GB	Not a special GB!

- Tilt boundary. Rotation axis ( $\mathbf{n}$ ) is in the boundary plane.
- Twist boundary. Rotation axis is normal to the boundary plane.

A symmetric twin boundary can also be described as a twist boundary or a tilt boundary—the difference depends on which aspect of the symmetry we think is most important. Not all twin boundaries are parallel to a mirror plane.

There are two well-known models of GBs that were developed primarily from studies of metals by considering the relative misorientation of the adjoining grains. These are the coincidence-site lattice (CSL) theory and the displacement-shift-complete lattice (DSCL). We first define two special quantities  $\Sigma$  and  $\Gamma$ . Imagine two infinite arrays of lattice points (one array for each crystal): they both run throughout space and have a common origin. For certain orientations, a fraction of the points in each lattice will be common to both lattices.

We call this fraction  $\Sigma^{-1}$ . (Then  $\Sigma$  is always an integer.) The lattice made up by these points is called the coincident-site lattice or CSL. The CSL is a lattice of common lattice sites, not common atoms.

If you translate one grain relative to the other,  $\Sigma$  is not changed.

### The Idea of $\Sigma$

It is easiest to understand these concepts by looking at simple illustrations as shown in Figure 14.1 for both  $\Sigma = 3$  (for  $\text{Al}_2\text{O}_3$ ) and  $\Sigma = 5$  (for  $\text{MgO}$ ). (Look back to Chapter 6 for the crystal structures.) The  $\Sigma = 3$  diagram shows two twin-related unit cells with the lattice sites identified. Overlapping these two cells produces the pattern in the shaded box and you can see that one in three lattice sites are common to the two grains (the ones at the corners of the box). The CSL for  $\Sigma = 5$  (just the lattice sites are shown) is also identified in the shaded box. Note that we must take account of both ions in considering the actual structure (see later). Sometimes it appears that the most valuable feature of the CSL model is that it gives a shorthand notation for talking about GBs. Low-angle boundaries are all  $\Sigma = 1$  GBs. Especially in ceramics, not all twin boundaries have  $\Sigma = 3$ . ( $\Sigma = 3$  occurs in face-centered cubic (fcc) crystals because the stacking of close-packed planes is ABCABC, so one in three planes is coincident across the twin boundary.) For a particular GB, if we choose any plane, then a certain fraction of points will lie on this plane in both lattices. We call this fraction  $\Gamma^{-1}$ . Again, it is easiest to appreciate the meaning of these definitions by studying the examples in the following sections.  $\Gamma$  is not widely used but might be the most important factor and it reminds you that the different planes may be

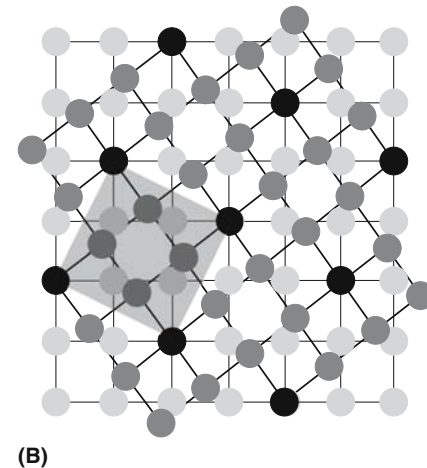
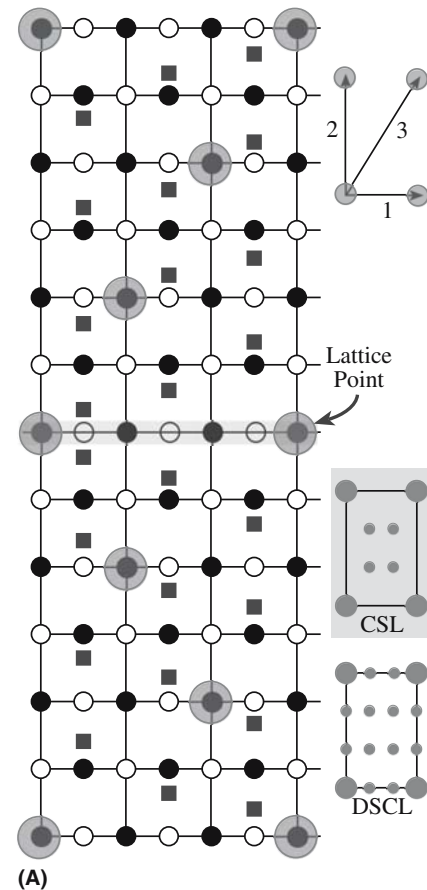


**FIGURE 14.1** Schematics of two low- $\Sigma$  GBs. (a)  $\Sigma = 3$ ; (b)  $\Sigma = 5$ .

very different.  $\Gamma$  can equal 1 for the  $\Sigma = 3$  GB, but could be 3, 9, or greater.

Throughout our discussion of GBs, you should keep in mind that there are many similarities to surfaces.

- There is a *pressure difference* across a curved GB just as there is across a surface.
- Charge affects the structure and chemistry of GBs.
- The structure of a GB determines its properties and behavior.
- GBs can be wet and dewet by GB films just as surfaces are by surface films.

Computer modeling of GBs can give considerable insights, but be careful when using older results in the literature. The complexity of ceramic structures and the Madelung problem cause difficulties and some older simulations may not be reliable, in part, because they used too little material in the calculation because of the capabilities of the computers.

We will discuss the properties of GBs later, but should keep in mind some features as we work through the chapter.

- The density of atoms in GBs is less than in the bulk crystal.
- The chemistry of a GB is not the same as the bulk (because the bonding must be different).
- Properties of GBs must differ from those of the bulk.

All GBs have a thickness (just like the soap films) and the GB is not uniform across that thickness; so GBs are actually volume defects again.

## 14.2 FOR CERAMICS

Ceramics are usually used in a polycrystalline form. GBs in ionic and covalent materials must be better understood to improve the science of processing of many modern ceramic materials; the properties of polycrystalline ceramics depend directly on the geometry and composition of GBs. The types of GBs commonly found in ceramic materials range from situations in which the distance between the grains is  $\geq 0.1 \mu\text{m}$  and such grains are separated by a second phase (glass), to the basal twin boundary in  $\text{Al}_2\text{O}_3$ , which is atomically abrupt and potentially very clean.

We need to understand how the presence of glass affects GBs in crystalline materials. This glass can be present on the surface of grains or within GBs as an intergranular film (IGF) in either single-phase materials or in materials with an intentionally high (or unavoidable) glass content.

The type of GB present in a sintered (or hot-pressed) compact may be significantly influenced by the surface characteristics of individual particles before and during sintering. Obviously if there is glass on the particle, there is likely to be glass in the GB. We need to understand the behavior of the surface at high temperatures under conditions appropriate to sintering (Chapter 24). Since GBs can be structured or can contain a thin noncrystalline layer, the chemistry of the region close to the GB is important.

We start by asking what is special about GBs in ceramics? This is the question we asked about surfaces and dislocations and the answer is basically the same.

- Ceramics have localized charge or covalent bonds. Dangling bonds exist at GBs.
- Since the bonding is ionic, covalent, or mixed ionic/covalent, there may be large local changes in density at the interface. Ceramic GBs have a space charge.

- Since the unit cells of all but the simplest binary compounds are large, it is likely that a GB with a fixed misorientation angle and interface plane will probably (rather than possibly) exist in more than one (meta)stable configuration. There will still only be one minimum energy.
- Energy is dependent on the GB plane, just as it is for surfaces. Accordingly, steps and facets (large steps) on these GBs will also be important. They are actually necessary for the GB to move.
- Many ceramics are processed in the presence of a second or third phase far away from conditions of thermodynamic equilibrium, and a remnant of this phase may remain at the GB even if it is not the lowest-energy configuration. Impurities segregate to GBs as illustrated by the XEDS and EELS plots in Figure 14.2.
- There is the problem of specimen preparation for analysis of interfaces in ceramics. In general, we cannot prepare a sample without altering the GB in some way.

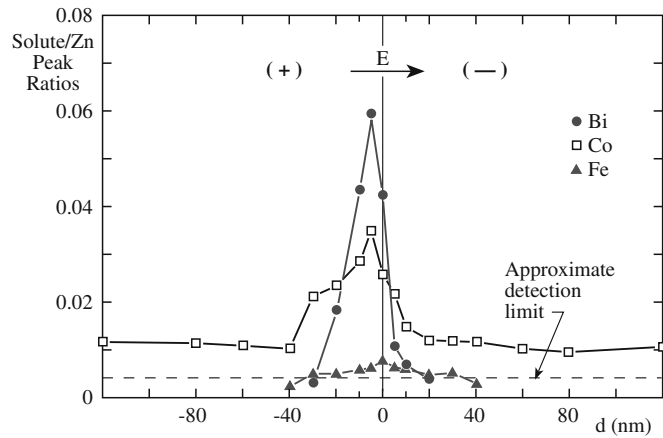
The extra difficulty is that we may never see a clean GB and, unlike surfaces, we have no way to clean one: ultrahigh vacuum (UHV) does not help us once the GB is there. What is different in comparison to metals? Metals try to make the density of atoms uniform due to the nature of the electron gas. GBs in ceramics may be much more open. The density of atoms in the GB can be very different from that in the bulk grains.

Is CSL theory important for ceramics? The CSL theory is relevant only when the adjoining grains are in direct contact. In ionic materials, we know that surfaces are almost never clean. Adsorption phenomena occur at internal interfaces as they do at surfaces. The driving force for segregation to GBs can be large. In fact, most GBs that have been studied have been “dirty.” Pure polycrystalline ceramic materials do not exist. The layer of glass that may be present at the GB is invariably associated with impurities. Such films are unusual in semiconductors (although they can exist) and would be exceptional in metals.

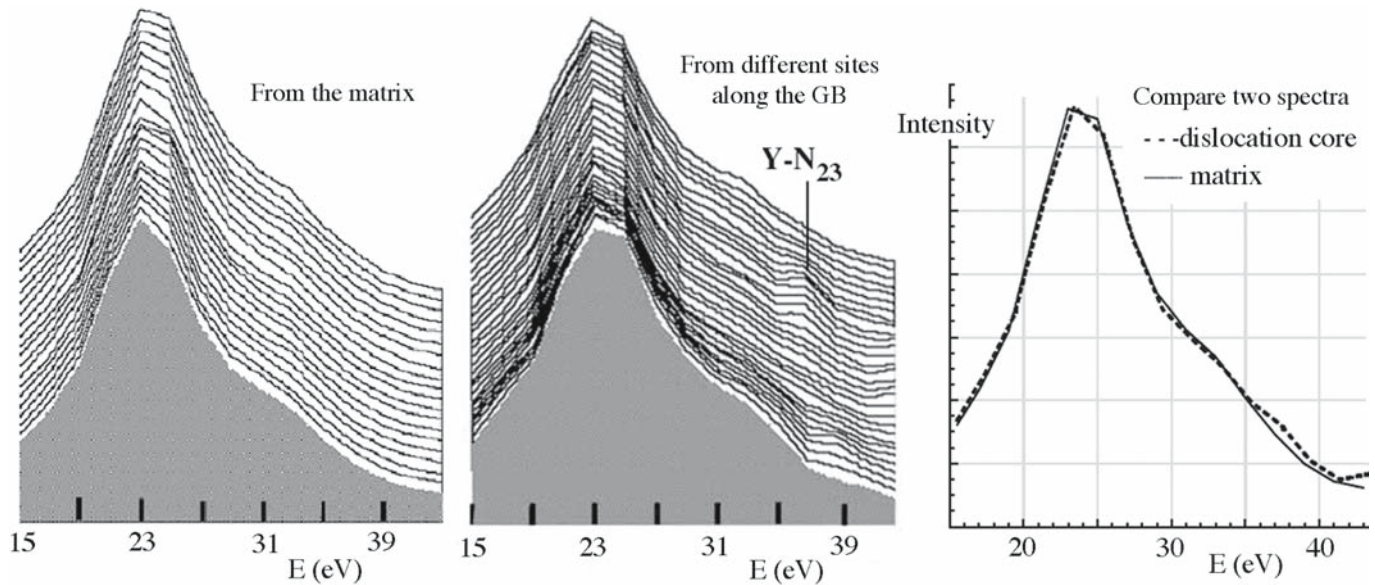
As with other materials, it is difficult to discuss so-called general GBs rather than special ones. Even special GBs in ceramics are not well understood. Both general and special boundaries are likely to be far less clean than models of such interfaces might assume. Methods for analyzing interfaces containing IGFs have been compared. It was concluded that the results can be ambiguous even when a combination of techniques is used. Unambiguous characterization will be achieved only when the structure, chemistry, and bonding are assessed simultaneously.

What *facts* are actually known about GBs in ceramics? We can make the following statements.

- *Structured GBs do exist in ceramic materials.* This conclusion applies to both high- and low-angle GBs.



(A)



(B)

**FIGURE 14.2** Solute distribution at GBs. (a) Profiles using XEDS; (b) EELS spectra used to analyze a GB in sapphire. In (a) the integrated X-ray solute/Zn peak ratios are plotted against  $d$ , the distance from the GB.

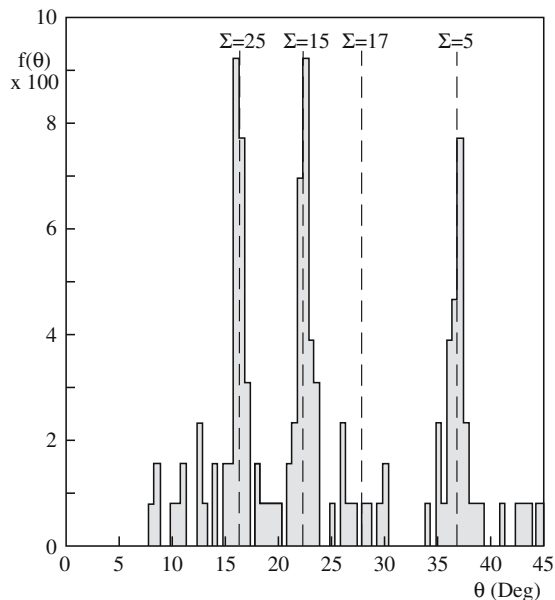
- GBs in ceramic materials do exist that are not “structured” but are, instead, wet over their entire area by an amorphous phase (an IGF).
- The structure of GBs in ceramic materials tends to be relatively more open (less dense) than is found for interfaces in metals that are otherwise crystallographically similar.
- The effects of several ions being present in the unit cell can be recognized. They can produce special interfaces in which only one sublattice is affected or can cause a modification of the interface structure itself.
- A particular interface may not have a unique structure because of the presence of two ions or because two or more structures are possible that do not have significantly different energies. It is also likely that the presence of impurities at the interface will modify the structure by favoring different polyhedral sites.

### 14.3 GB ENERGY

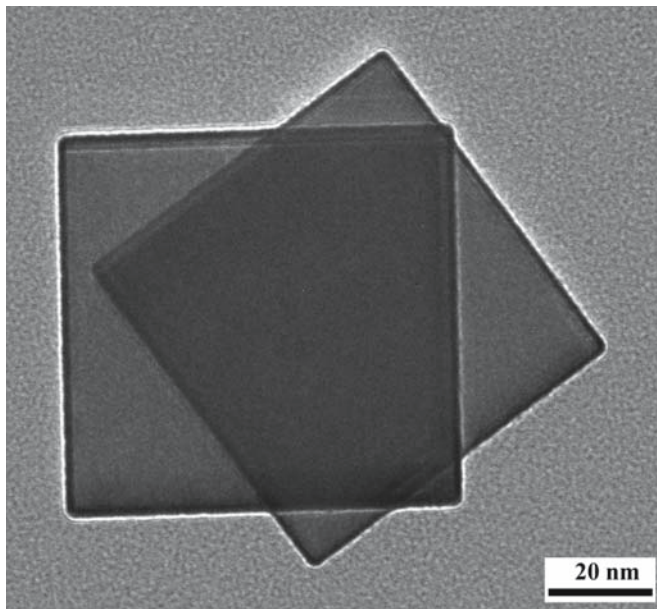
The energy of a GB is a very important quantity, but it is even less well known than for surfaces, and is usually determined in relation to surface energies. There are two key questions:

- How do we define the energy of a grain boundary?
- What factor causes a GB to have a low interfacial energy?

The GB energy,  $\gamma$ , depends on the misorientation of the two grains and on the orientation of the plane. We can again use the Wulff plot ( $\gamma$  versus  $\theta$  where  $\theta$  now means the misorientation) and the inverse Wulff plot ( $\gamma^{-1}$  versus  $\theta$ ). The challenge of  $\gamma$  versus  $\theta$  plots is to define the orientation of the GB plane, i.e., having fixed  $\theta$ , you must still fix  $\mathbf{n}$ , the GB normal for both grains. Keep in mind



(A)



(B)

**FIGURE 14.3** Rotated MgO nanoparticles and their relation to  $\Sigma$ . The frequency of measuring a rotation  $\theta$  is  $f(\theta)$ .

that we expect  $\gamma$  to decrease as the temperature increases as is found for surfaces (Eötvös rule); this dependence on temperature will be important in sintering. One approach to the problem is to plot the individual Wulff plots for the two separate grains and then to consider what happens when the two grains are joined along a particular plane.

### MgO Smoke

One method used to examine the possibility of low-energy GBs is the classic MgO smoke experiment. Mg metal is burned in air and the resulting MgO smoke particles are caught on a grid. The relative orientations between cube

particles can be determined using TEM; the angles between different  $\{001\}$  planes are measured much as Haüy originally did for single crystals. We now do this more accurately using diffraction patterns or high-resolution transmission electron microscopy (HRTEM) images. This experiment is special for ceramics because we are joining nanoparticles at high temperatures although we do not actually know when they joined so we do not know the sintering temperature. Figure 14.3 shows an example of such particles together with the frequency of occurrence,  $f(\theta)$ , of the misorientation angle. The oxide bicrystal particles form with a strong preference for certain orientations in which the two crystals have a fraction of their lattice sites in common: the coincidence boundaries. This experiment has long been one of the bases for believing that  $\Sigma$  is an important parameter in determining the energy of GBs. It does not measure  $\gamma$  but does suggest that  $\gamma$  is related to  $\Sigma$ . Unfortunately, results from computer modeling suggest that this is not necessarily the case, but it is such an attractive intuitive concept that it persists.

### Energy of Low-Angle GBs

When  $\theta$  is small, the energy of a low-angle GB is approximated as the total self-energy of the dislocations within a unit area of the boundary. However, as  $\theta$  increases the stress fields of the dislocations progressively cancel out so that the energy increases at a decreasing rate and may peak before decreasing to a low value at a special orientation as shown in Figure 14.4. When the dislocation spacing is small, the dislocation cores overlap, so that when  $\theta$  exceeds  $10^\circ$  (somewhere in the range of, say,  $10\text{--}16^\circ$ ) it is not possible to identify the individual dislocations.

The Read–Shockley formula for the energy,  $E$ , of a low-angle GB considers the stress field and the core energy of the dislocations.

$$E = E_0\theta(A - \ln\theta) \quad (14.1)$$

$E_0$  is a constant that is a function of the elastic properties of the material (and hence of the stress field) and  $A$  is a

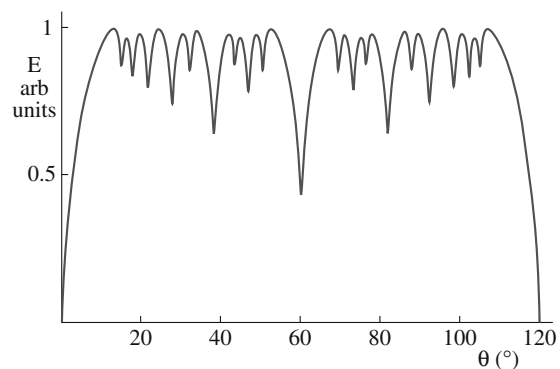


**FIGURE 14.4** Cusp in a plot of GB energy versus misorientation angle,  $\theta$ .

constant that depends on the core energy (remember our discussion of  $r_0$ , the dislocation core radius).

We can also define the Gibbs adsorption isotherm for grain boundaries. We extend the analysis from surfaces to the internal interface.

$$\frac{\partial \gamma}{\partial \mu_i} = -\Gamma_i \quad (14.2)$$

where  $\Gamma_i$  is the excess moles of  $i$  per unit area of the GB. All the other variables (e.g.,  $P$  and  $T$ ) are held constant.

## 14.4 LOW-ANGLE GBs

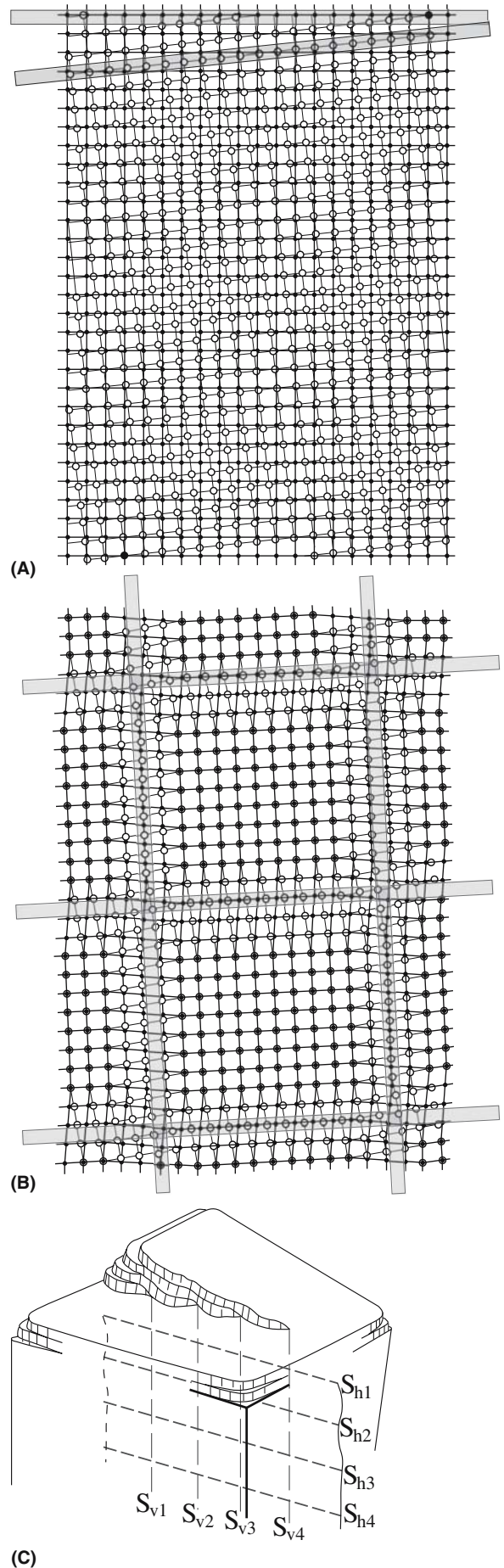
Low-angle GBs contain arrays of dislocations. In its simplest form, the structure of the twist boundary consists of two sets of orthogonal screw dislocations as shown in Figure 14.5a and b; the schematics show the structure before and after relaxation to form the screw dislocations. Figure 14.5c shows how dislocations in a twist boundary might be seen emerging at the surface; you can see that part of the grain is physically twisted relative to the other because of the screw dislocations. The simplest tilt GBs consist of one set of edge dislocations as shown in Figure 14.6. Note that the statements both include the word “simplest.” Most tilt boundaries will have two different sets of edge dislocations, and twist boundaries in noncubic materials may be accommodated by only one set of dislocations! Figure 14.6b shows that we must use two sets of edge dislocations if the GB is not symmetric. (We sometimes have to, even if it is symmetric.)

Figure 14.7 is a TEM image of a twist boundary in Si; a tilt boundary in NiO is shown in Figure 14.8. The image of this tilt boundary is particularly interesting because it shows that the density is different at the GB.

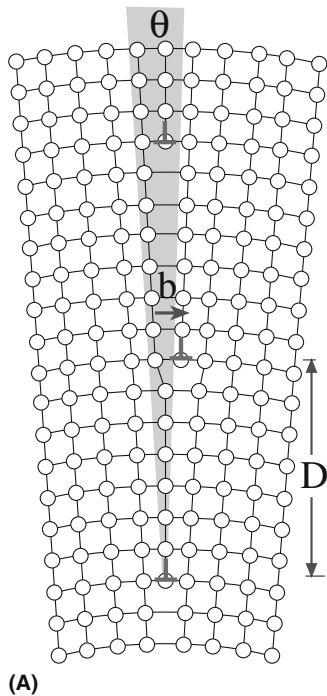
The spacing of the dislocations,  $D$ , is related to the boundary misorientation angle,  $\theta$ , and the Burgers vector of the dislocations,  $b$ .

$$D = \frac{b/2}{\sin \theta/2} \approx \frac{b}{\theta} \quad (14.3)$$

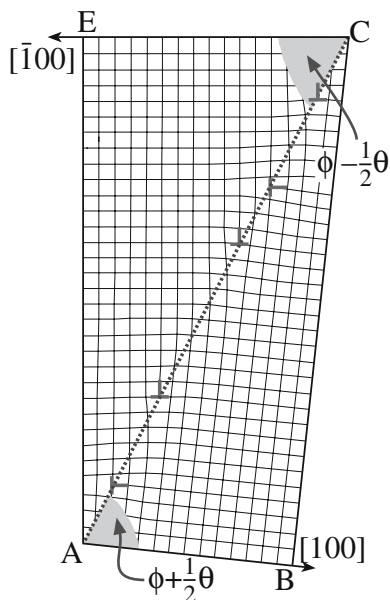
The latter relation holds only if  $\theta$  is very small. In this case, we can either reveal the individual dislocations by decorating them or by etching the surface as shown in Figure 14.9. Equation 14.3 has been well tested for fcc metals and some simple ceramics.



**FIGURE 14.5** Schematics of a low-angle twist GB. (a) Before and (b) after local atomic relaxations. (c) The twist when the GB emerges at the surface.



(A)



(B)

**FIGURE 14.6** Schematics of low-angle tilt GBs. (a) Symmetric; (b) asymmetric.

The structure of dislocations and interfaces in ionic and covalent materials has been the subject of much theoretical and experimental research, motivated in part by the realization that the extensive body of information and the concepts that have been accumulated for metallic systems cannot necessarily be directly transferred to these nonmetallic systems.

The structures of all defects in ceramic materials can be more complex than those of similar defects in the more thoroughly studied pure metals because of the presence of two or more ionic species on two sublattices. The implica-

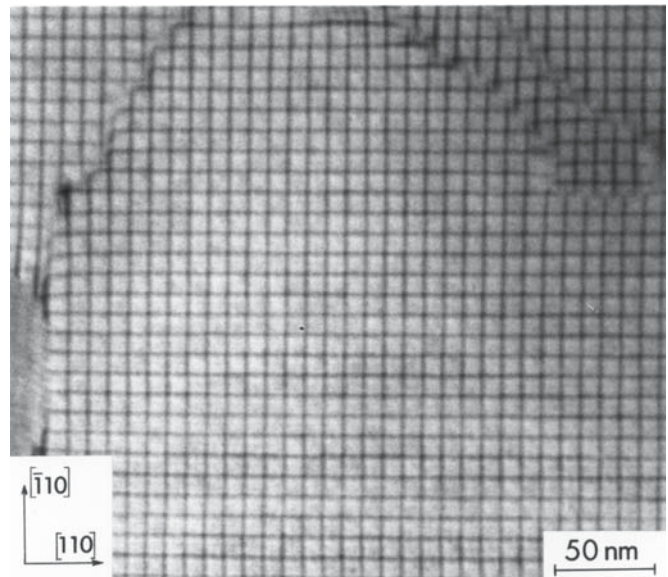


**FIGURE 14.7** Two sets of orthogonal screw dislocations in a low-angle (001) twist GB in Si.

tion of the presence of two types of ions is well known in ceramics since it results in the phenomenon of dissociation by climb of dislocations in the lattice or in the GB. The phenomenon has been recorded for materials such as spinel,  $\text{Al}_2\text{O}_3$ , and garnet. Actually, this phenomenon can also occur in more complex metallic, ordered alloys for precisely the same reason. In  $\text{Al}_2\text{O}_3$  and  $\text{MgAl}_2\text{O}_4$  the partial dislocations created by the dissociation process are “perfect” dislocations of the oxygen sublattice; the stacking fault thus formed is therefore only a fault on the cation sublattice.

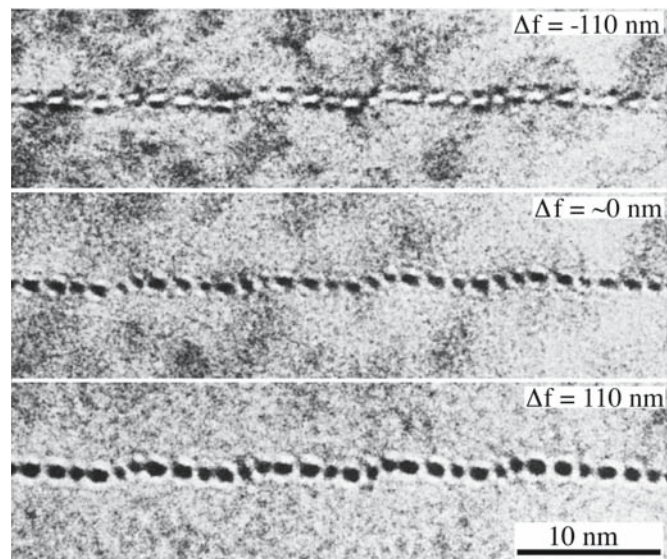
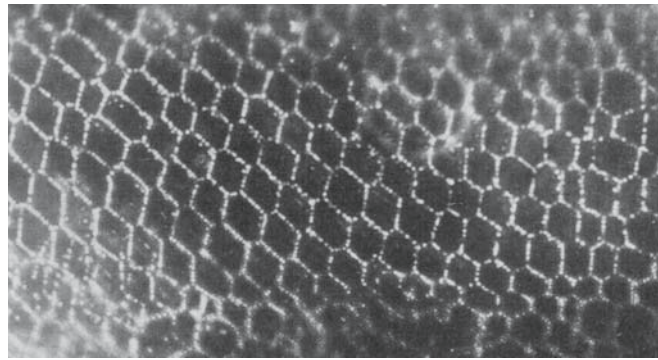
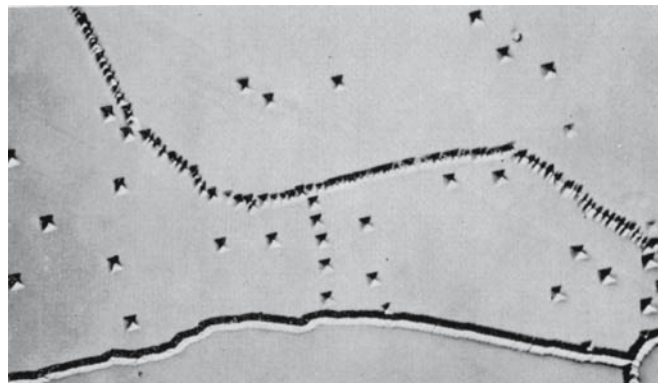


**FIGURE 14.8** Dislocations in a low-angle tilt GB in NiO. The defocus ( $\Delta f$ ) images show a change in density at the dislocation cores.



(A)



(B)

**FIGURE 14.9** Seeing low-angle GBs by (a) decoration (silver particles on a GB in KCl) and (b) etch pits (LiF).

The effect of the large unit cell is well illustrated by the low-angle 111 twist boundary in  $\text{MgAl}_2\text{O}_4$ . The (111) interface plane can be chosen as A or B in the schematic of the crystal

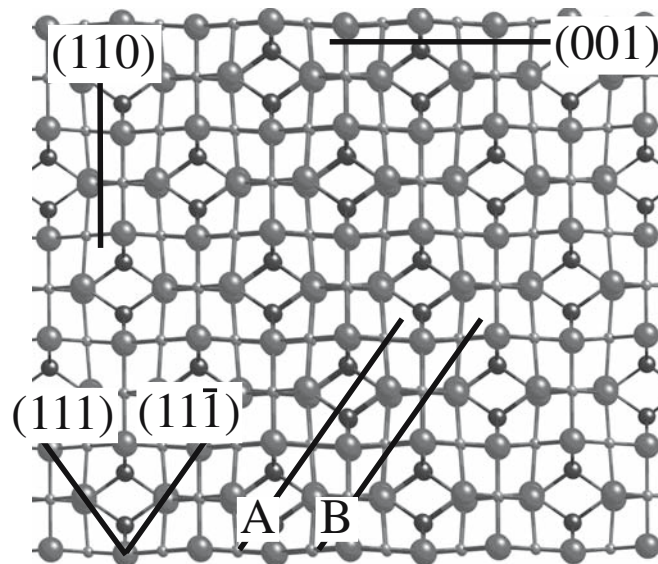


**FIGURE 14.10** Spinel structure projected along  $\langle 1\bar{1}0 \rangle$  summarizing the important crystallographic planes. A and B are parallel but structurally different (111) planes.

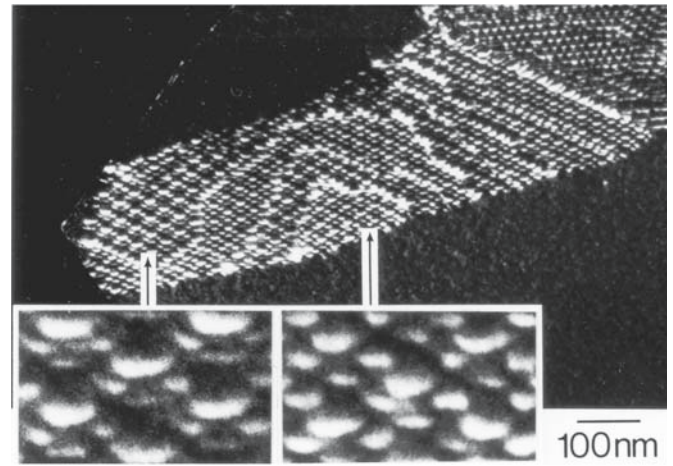


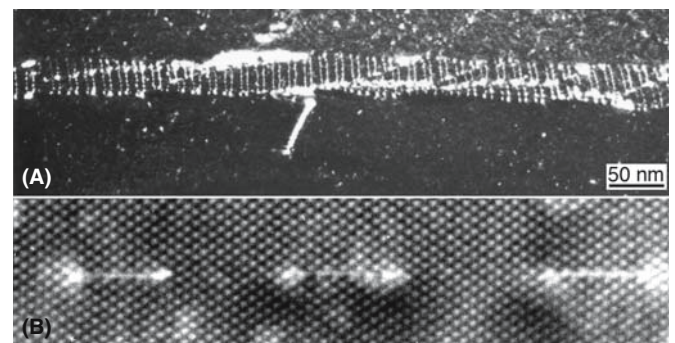
**FIGURE 14.11** Low-angle {111} and {001} twist GBs in spinel showing two structures in each case.

structure shown in Figure 14.10. In the spinel (111) twist boundary, an  $\frac{a}{2}[1\bar{1}0]$  screw dislocation can dissociate on the (111) plane into two parallel  $\frac{a}{4}[1\bar{1}0]$  screw partial dislocations. (Because  $a$  is large and this dissociation produces dislocations that would have been perfect if we considered only the O ions.) Since the self-energy of a dislocation is proportional to  $b^2$ , this dissociation halves the total dislocation self-energy. The partial dislocations are separated by a stacking fault (SF), but the energy of this fault depends on whether the glide plane of the plane of the stacking fault is A or B. Thus, there are two different SFs on a {111} plane and two different stacking fault energies (SFEs). The consequence of this multiplicity in the value of the SFE is illustrated in

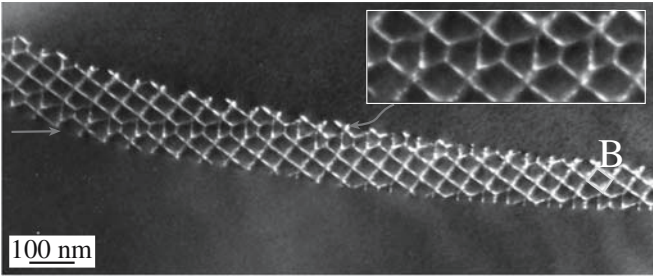
Figure 14.11 where the width of the SF takes on two distinct values for both GBs.

Figure 14.12 shows the climb dissociation of edge dislocations in a spinel tilt boundary. (This is just an extension of Figure 12.15.) In Figure 14.13 we can see a so-called extrinsic dislocation (along [100]) interacting with the

width of the SF takes on two distinct values for both GBs.



**FIGURE 14.12** A low-angle tilt GB in spinel showing an array of climb-dissociated edge dislocations. (a) The GB viewed at an angle; (b) at higher magnification, the dislocations viewed end-on.



**FIGURE 14.13** An extrinsic dislocation interacting with a low-angle {001} twist GB in spinel. Note how all the dislocations are changed by the interaction as seen in the enlarged inset.

screw dislocations that are already present in the interface (to accommodate the twist) in the (001) twist GB.

### 14.5 HIGH-ANGLE GBs

When  $\theta$  is  $>10^\circ$ , the interface is referred to as a high-angle GB. Figures 14.14 and 14.15 show schematics of the  $\Sigma = 5$  GB in NiO in the tilt and twist configuration, respectively, taking account of the presence of two ions. The situation is clearly complex: only the lower structure in Figure 14.14 could exist (the others have similarly charged ions too close together). The same considerations hold for the twist GB shown in Figure 14.15: when two ions of like charge are adjacent, one must be removed. As in the low-angle case, high-angle GBs can exist with more than one structure. Figure 14.16 shows images of two special GBs in ZnO; the difference between a symmetric high-angle GB

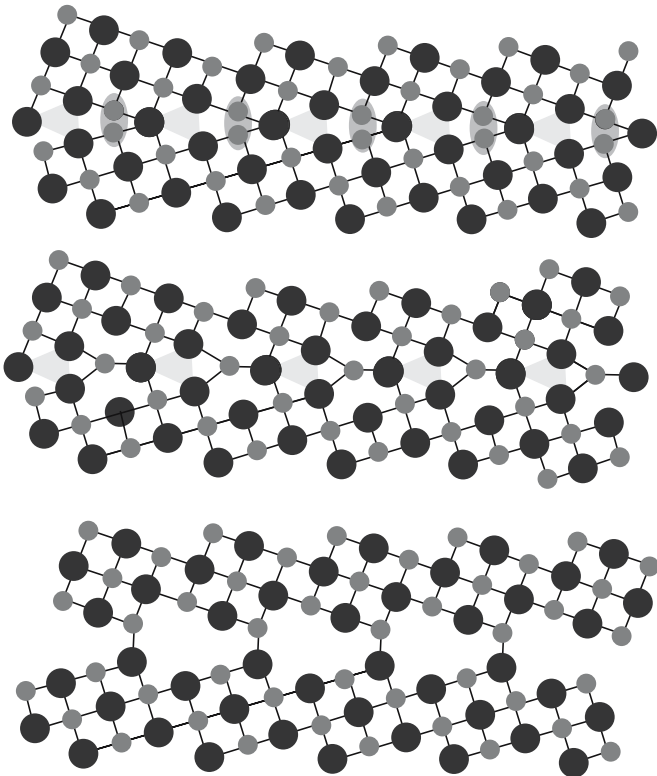


**FIGURE 14.14** Schematics of the [001]  $\Sigma = 5$  tilt GB in NiO; only the lower one is actually possible.

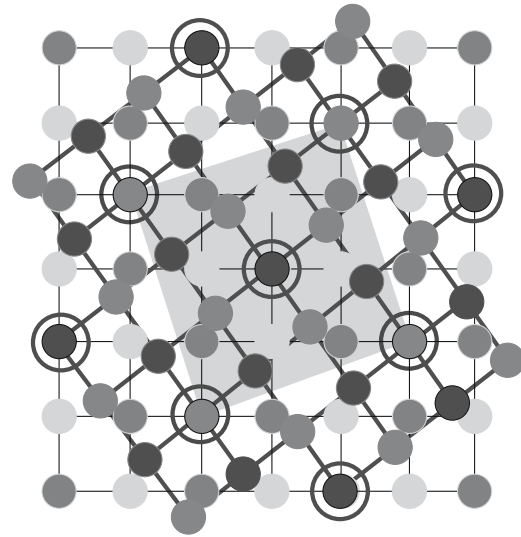


**FIGURE 14.15** Schematic of the (001)  $\Sigma = 5$  twist GB in NiO showing anions and cations. This structure cannot occur unless some ions are removed.

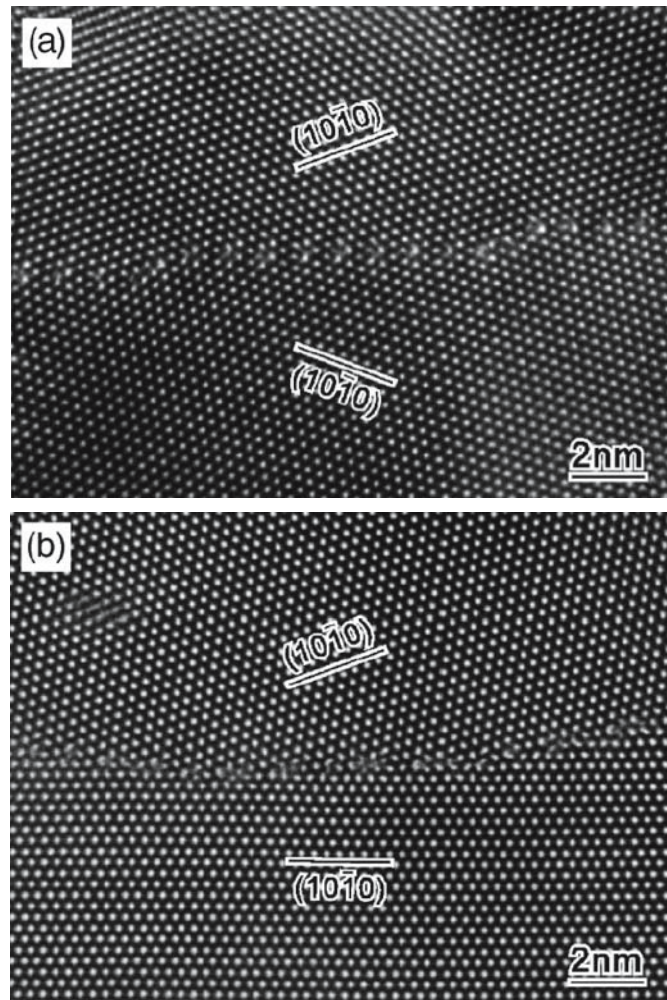


**FIGURE 14.16** HRTEM images of two high-angle GBs in ZnO: (a) near-symmetric; (b) asymmetric.

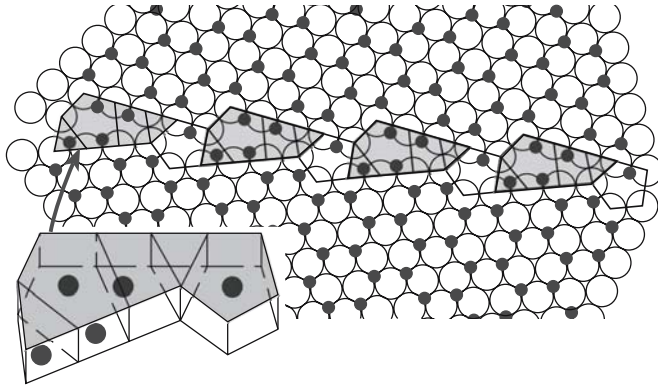


**FIGURE 14.17** Schematic of a GB in  $\text{Al}_2\text{O}_3$  showing the creation of new polyhedra in the GB. The inset shows a tilted view of the repeating group of polyhedra.

and the lower-angle asymmetric counterpart is striking; this type of asymmetric faceting often involves low-index planes as shown here. You can imagine why asymmetric units might be favored by examining Figure 14.17, which shows a schematic of a GB in  $\text{Al}_2\text{O}_3$ . Polyhedra that were not present in the perfect crystal in Chapters 6 and 7 can be present at a high-angle GB, and these can accommodate larger impurity ions than can the bulk.

More complex high-angle GBs have been the subject of far fewer studies, in part because of the experimental difficulties in characterizing them. This lack of information is unfortunate since these interfaces are ubiquitous in sintered materials. High-angle GBs formed by hot-pressing together two single crystals of MgO appear to behave as would have been anticipated from studies on the corresponding interfaces in fcc metals and semiconduc-

tors and support the earlier interpretation of experiments on MgO “smoke.” However, such interfaces have been the subject of extensive computer-modeling studies that often give a contradictory view.

As these observations show, the plane adopted by a high-angle GB is a very important factor. Such GBs in ceramic materials show a particularly strong tendency to facet, so the plane must be important. These facet planes are almost invariably parallel to low-index planes in one or both grains. The basic argument is that low-index planes are the most widely separated planes and thus involve less energy when a “stacking error” is present in the crystal.

A particularly striking illustration that makes us question the importance of  $\Sigma$  as a measure of the energy of a GB is provided by observations of the  $\Sigma = 99$  and  $\Sigma = 41$  boundaries in spinel, where, by chance, the interface can facet parallel to several pairs of (different) low-index planes in both grains simultaneously. A similar situation exists for phase boundaries. It could be that the faceting onto low-index planes would lower the energy to below that of similar GBs having a lower  $\Sigma$ . There are no atomistic calculations for such GBs.

## 14.6 TWIN BOUNDARIES

As in metals, twin boundaries are common in many ceramic materials including MgO, spinel,  $\text{Al}_2\text{O}_3$ ,  $\text{Fe}_2\text{O}_3$ , the rare earth oxides, quartz, Si, and, of course, the new high-Tc superconductors. Indeed, it seems certain that such interfaces will occur in all crystalline ceramic materials. Some special twin relationships observed in minerals are illustrated schematically in Figure 14.18. The

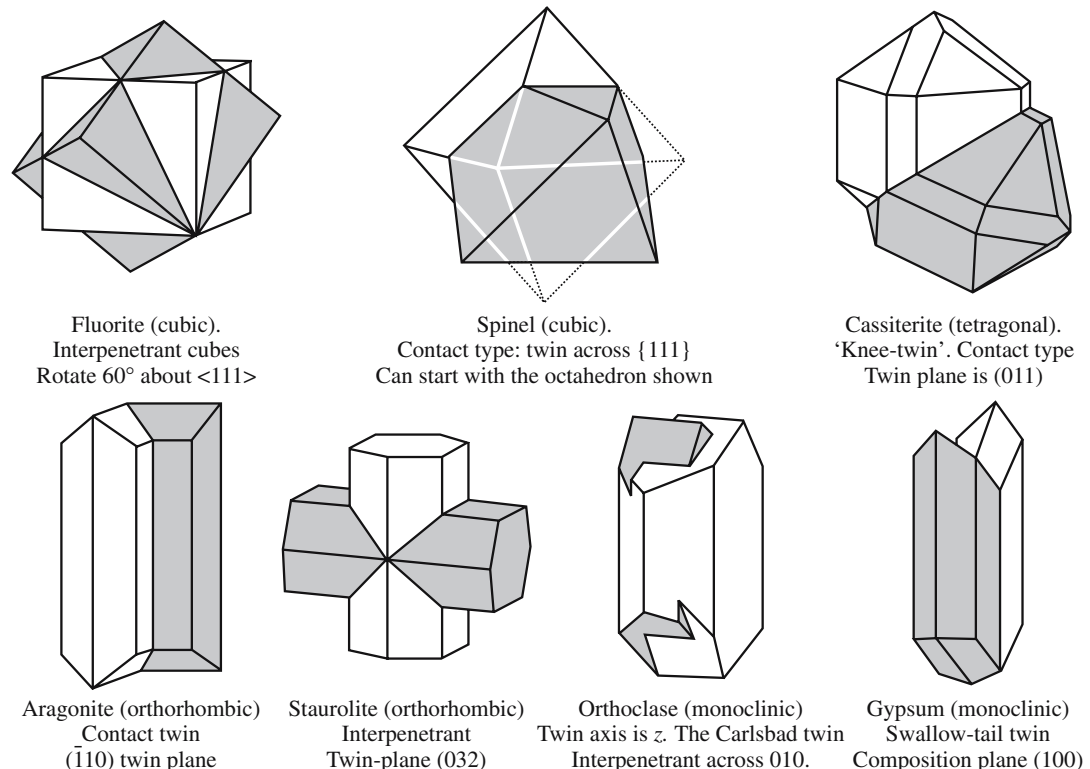


**FIGURE 14.18** Examples of twinned grains found in different minerals.

observation of so many twin boundaries is interesting because they are found to facet parallel to low-index planes in at least one grain. We noted that such interfaces can accommodate impurity ions, and this can lead to the phenomenon of chemical twinning, wherein apparently different crystal structures can be related to one another by the periodic repetition of a pair of twin interfaces. This concept can be used to understand the actual mechanism of a phase transformation in a ceramic system.

Several different types of twin boundaries have been seen in  $\text{Al}_2\text{O}_3$ ; the basal twin boundary is the  $\Sigma = 3$  GB, which was discussed in Figure 14.1a. We can form a variety of twin boundaries in  $\text{Al}_2\text{O}_3$  by mirroring the structure across low-index planes that are not mirror planes in the perfect crystal; hence the  $(\bar{1}102)$  plane, the  $(\bar{1}104)$  plane (illustrated in Figure 14.19), and the  $(11\bar{2}3)$  plane all give twin boundaries [as does the  $(0001)$  plane, of course]. A rhombohedral twin boundary [the  $(10\bar{1}2)$  twin boundary] is shown in Figure 14.20; notice that it is faceted.

All interfaces in spinel, even the  $\Sigma = 3$ ,  $(111)$  twin boundary, can exist with at least two different structures. In a formal treatment of such interfaces the different structures considered here can, in principle, be described by choosing different rigid-body translation vectors. However, such translations are not the small relaxations familiar in, for example, the  $\{112\}$  lateral twin boundary in Al, but are more closely related to stacking faults in fcc metals. The image illustrated in Figure 14.21 shows two parallel  $\{111\}$  twin boundaries (separated by a microtwin). The translations at the two twin boundaries are different as you can see in the insets.

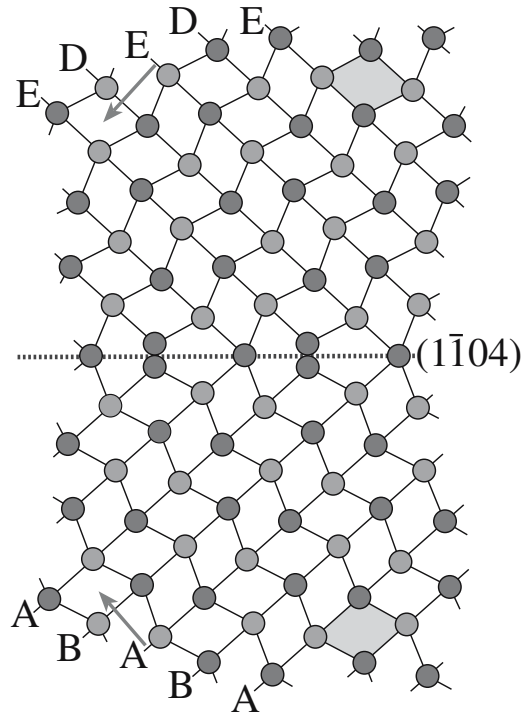
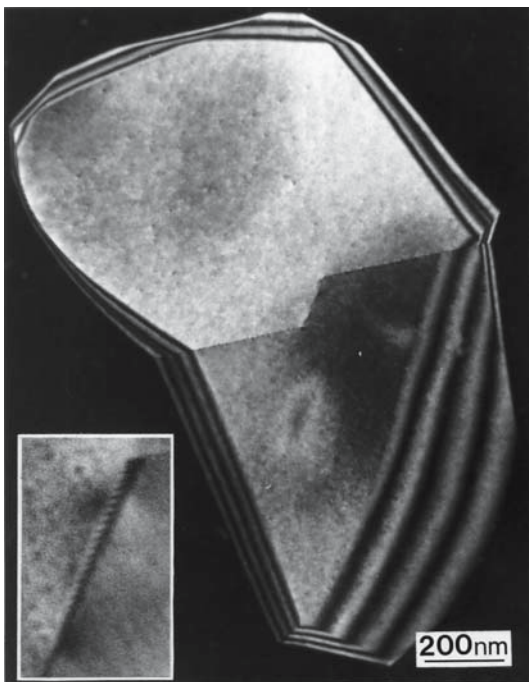


**FIGURE 14.19** Schematic of a  $(\bar{1}104)$  twin boundary in  $\text{Al}_2\text{O}_3$ . The arrows show the  $\langle 0001 \rangle$  directions; the letters show the hcp stacking of the anions. The cations are omitted but sit in the octahedral—shown by the shaded rhombi.

This translation, which is parallel to the  $\{111\}$  plane, is seen because of the location of the cations. As far as the oxygen sublattice is concerned, the twin interface is actually a mirror plane: it is just like the  $\{111\}$  twin boundary in fcc Cu.

### THE TWINS

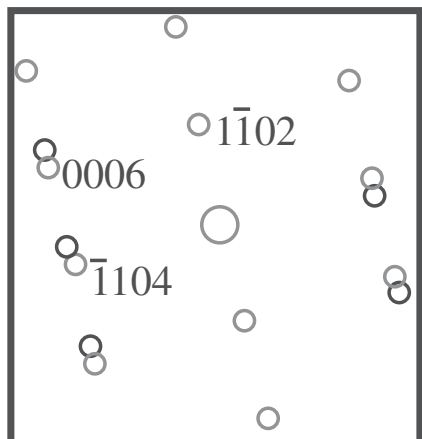
A twin is a grain; a twin boundary is a GB.



(A)



(B)



(C)

**FIGURE 14.20** Rhombohedral twin boundary in  $\text{Al}_2\text{O}_3$  and its diffraction pattern.

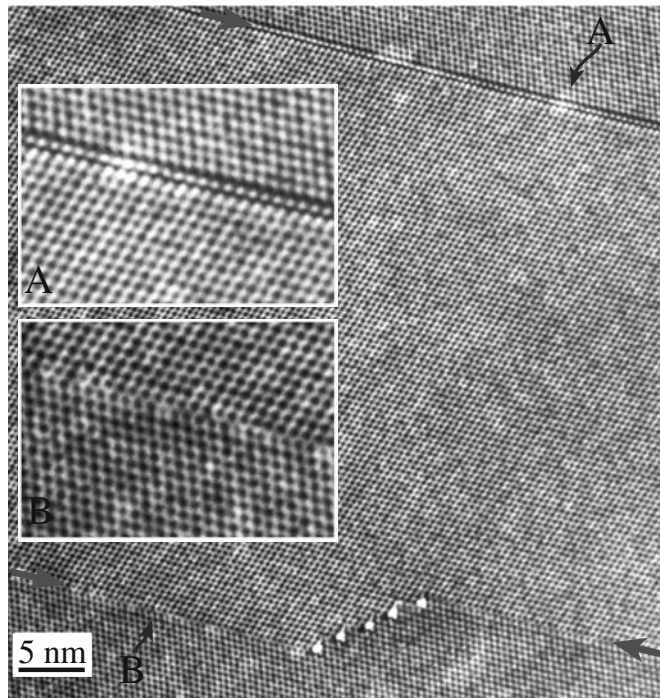


**FIGURE 14.21** Two parallel  $\{111\} \Sigma = 3$  twin boundaries in spinel having different structures (identified by the arrows). The insets show regions A and B at higher magnifications.

The lateral  $\Sigma = 3$  twin boundary in spinel is also special. The structure of this interface can be entirely described in terms of  $\{111\}$  segments (which may have different structures, as noted above) and triangular-prism channels, which lie along  $\langle 110 \rangle$  directions and are observed as white spots in HRTEM images. The faceting consists entirely of ordered (aligned) arrays of these prism columns; the interface shown here is actually dislocation free, although the prisms can be modeled as an array of dislocation dipoles. There was no local strain contrast in the TEM image.

The image shown in Figure 14.22 is from a thin film of NiO and reminds us that GBs that correspond to a special twin orientation are not necessarily flat. In that case, they are probably more similar to other high-angle boundaries. The twin boundaries in the NiO film occur because NiO can grow on a basal-alumina substrate in two twin-related orientations. We see the twin boundaries because the density is lower at the GB.

An example of how twins can form in a more complex system is shown schematically in Figure 14.23 for aragonite. This figure shows the  $\text{CO}_3^{2-}$  anions as triangles (as we saw in calcite) while the closed circles represent  $\text{Ca}^{2+}$  ions. (The numbers give heights of ions in the cells and serve to emphasize the twin symmetry.)

A special group of closely related oxides is illustrated in Figure 14.24. These oxides consist of blocks of  $\text{MO}_6$  octahedra (seen as squares along the cube direction), which can be shifted parallel to certain crystallographic planes (known as shear planes) to produce new structures.

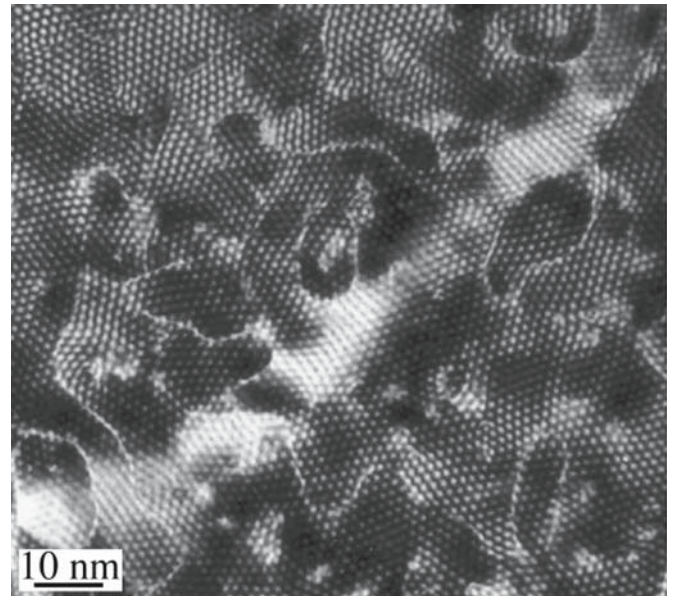


**FIGURE 14.22** Curved twin boundaries in a thin film of NiO on an  $\text{Al}_2\text{O}_3$  substrate. (The hexagonal pattern is a moiré interference effect.)

The circles are tetrahedral cations. Essentially, the shearing acts to change the chemistry along that plane. Crystallographic shear planes are thus like regular stacking faults, but the chemistry also changes—they are *chemical stacking faults*. An example of  $\text{WO}_{3-x}$  encapsulated in  $\text{WS}_2$  is shown in Figure 14.25.

Twin boundaries, like other GBs, can accommodate new ions so that the chemistry changes along the twin

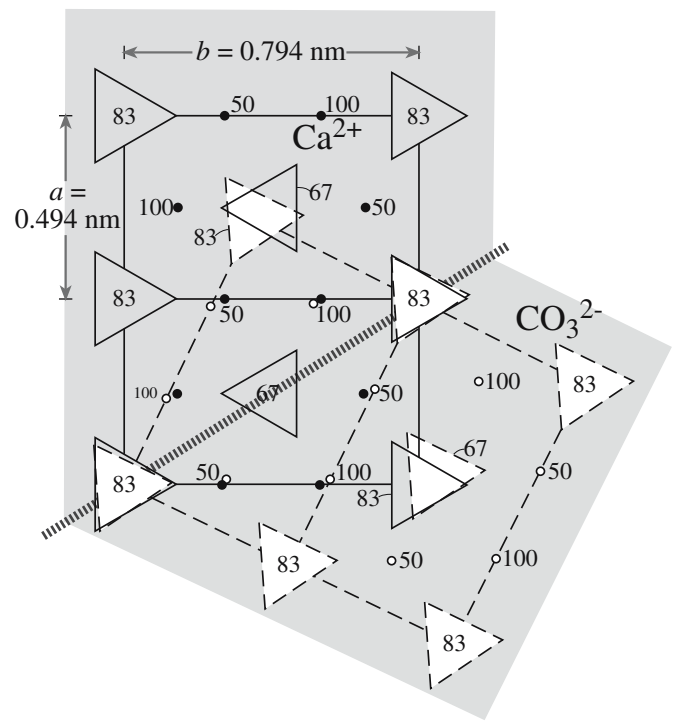


**FIGURE 14.23** Mimetic twinning in aragonite. This gives rise to trilling twins when the operation is repeated.

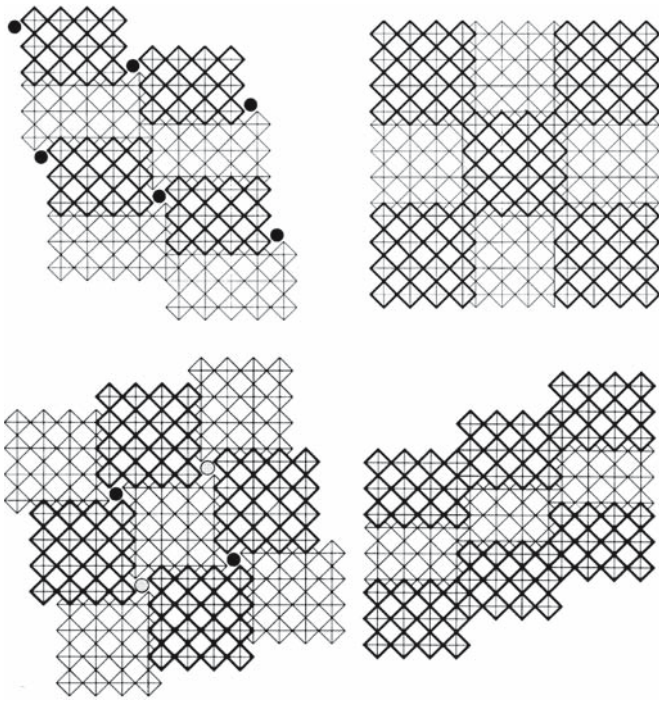


**FIGURE 14.24** Shear planes in  $\text{WO}_3$ . Dark and light lines are at heights 0 and 0.5.

plan. A periodic repetition of alternating twin planes, each of which accommodates ordered impurities, can then give rise to a new structure. This process is known as chemical twinning. The result for  $\beta'''$ -alumina is illustrated in Figure 14.26. Planar defects can readily be incorporated into this

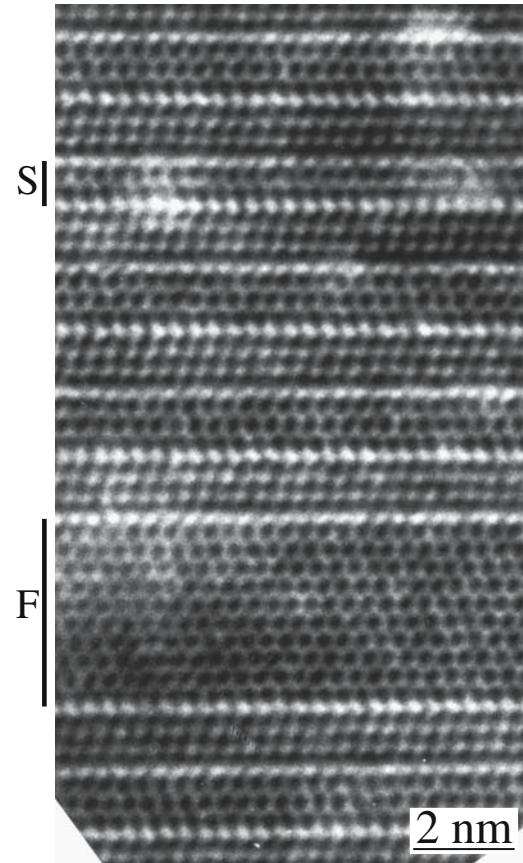


**FIGURE 14.26** The structure of  $\beta'''$ -alumina as a repetition of chemical twin boundaries. S and F are a block of spinel and an SF, respectively.

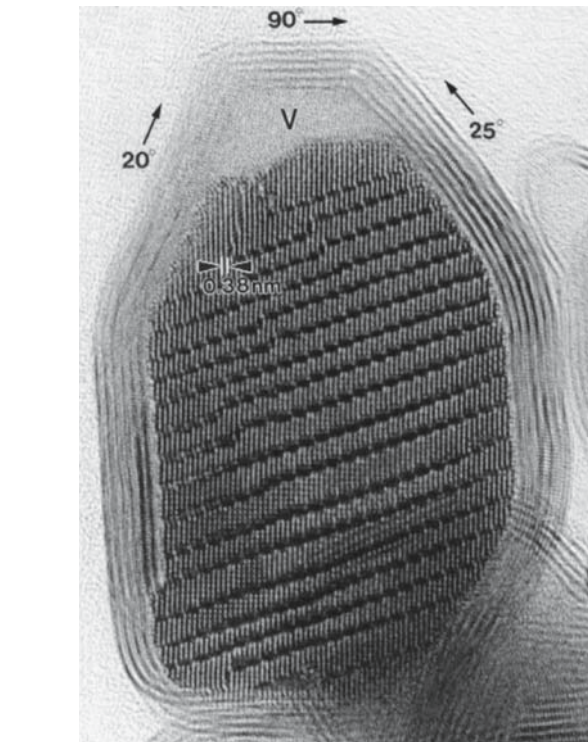


**FIGURE 14.25** A defect W oxide encapsulated in a fullerene.

structure. This particle of  $\beta'''$ -alumina contains a sheet of spinel; the spinel is like a sheet of a second phase. As we have seen in Section 7.12, we can also think of the structure of the  $\beta'''$ - $\text{Al}_2\text{O}_3$  as being blocks of spinel that twin on every six  $\{111\}$  oxygen planes. The attractive part of this description is that we can then understand the fault in the structure where the twin occurs after only four  $\{111\}$  oxygen planes. Remember that the twin planes are not actually spinel twin planes because the chemistry is different on the twin plane.

## 14.7 GENERAL BOUNDARIES

General boundaries may be curved with no specific value of  $\Sigma$ . Can we determine if the GB is clean or what its structure is? We can know if it is not clean and put an upper limit on the impurity content, but we still will not know its structure.

The relationship between the physical parameters of any individual interface and the mechanical strength or properties of that interface has not been directly determined for any ceramic material. As with many

properties of ceramic materials, measurements on GBs are likely to be controlled by dopants or impurity phases; the latter may be present at the 10% level. Computer modeling is usually carried out for pure materials. Finite element modeling (used for fracture studies, crack initiation and propagation, etc.) generally makes assumptions regarding the elastic parameters, which may be very different at an impure interface in comparison to bulk material; the bonding at the interface is different, so the elastic properties must be different too.

## 14.8 GB FILMS

In Chapter 13 we discussed how a liquid behaves on a solid surface if the solid is not inert. We noted that the situation could change due to evaporation at high temperatures and that the wetting phase need not be a liquid to wet or dewet.

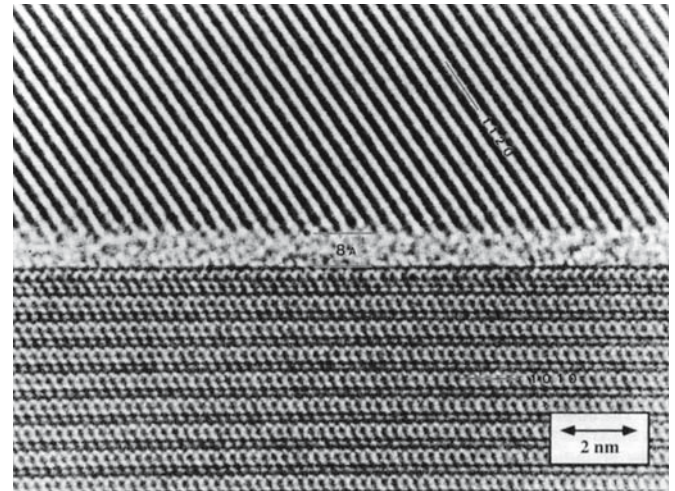
- GB films are directly analogous to films on surfaces or substrates.
- How thick must a film be before it is a new phase?
- Is a GB containing a film one interface or two?

The simple view of whether a glass film will be energetically favorable is that if  $2\gamma_{sl} < \gamma_{GB}$ , then the film is preferred. This statement is too simplistic, in part because GB films are unlikely to be uniform across their thickness. If  $\gamma_{sl}$  is  $\sim\gamma_{GB}$  then we would expect the GB to be stable, but even in this case, the glass must go somewhere.

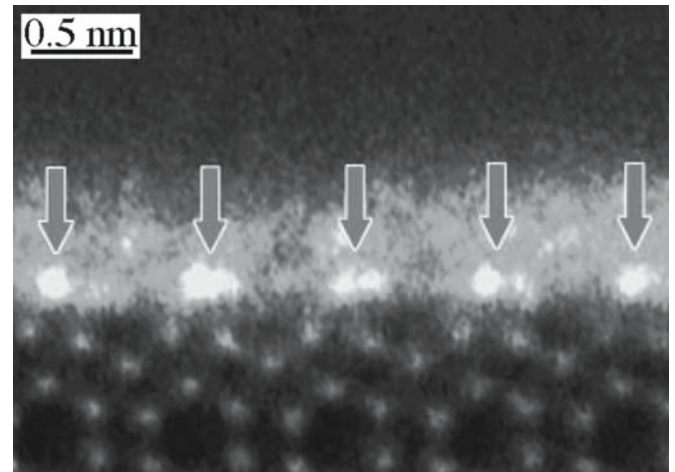
Any of the four types of GB could contain a GB film. How stable the film would be will clearly depend on the energy of the GB with the film versus without it and the availability of a mechanism for removing the film if this would lower the energy.

We know that liquid phases can be very important in polycrystalline ceramic materials. We also know that most interfaces in some ceramics (e.g.,  $\text{Si}_3\text{N}_4$ ) contain a very thin ( $\sim 1\text{--}5\text{ nm}$ ) IGF as illustrated in Figure 14.27. Thin amorphous layers have been reported to be present in a wide range of ceramic materials (see Table 14.1). It is sometimes incorrectly assumed that all GBs (other than special twin boundaries) in  $\text{Al}_2\text{O}_3$  contain such a thin amorphous film. In some materials the same interface may or may not contain an amorphous film, depending on how it was processed.

- Glass is very often present in ceramic materials whether intentionally included or not. In many oxides it is present because of impurities in the initial materials used to process the compact. In others it is intentionally



(A)



(B)

**FIGURE 14.27** Examples of HRTEM image of IGFs in  $\text{Si}_3\text{N}_4$ . (a) Phase-contrast image; (b) Z-contrast image showing ordering of rare-earth dopant at the glass/crystal interface.

added to lower the processing temperature via the process of liquid-phase sintering.

- The width of glassy GB films can vary from  $\sim 1\text{ nm}$  to  $>1\text{ }\mu\text{m}$ .
- The TEM techniques used to identify these films do not always give unambiguous results.
- At high temperatures the mechanical properties of a ceramic may be drastically lowered if a glass is present. For example, the viscosity of the glass decreases significantly at a relatively low temperature leading to enhanced creep and related phenomena; remember that the viscosity of soda-lime-silica glass varies from  $10^{15}\text{ dPa}\cdot\text{s}$  at  $400^\circ\text{C}$  to  $10^2\text{ dPa}\cdot\text{s}$  at  $1300^\circ\text{C}$ . At the higher temperature glass cannot support a shear stress and allows

**IGFs**

A note on very thin films: if a film is  $\sim 1\text{ nm}$  thick and the system is in equilibrium, then the film may be better described as an adsorbate layer. Experimentally, the challenge is knowing that the system is in equilibrium.

**TABLE 14.1 Examples of Intergranular Phases**

System	Property affected	Notes
Glass in $\text{Si}_3\text{N}_4$	Mechanical	Glass forms from components added as sintering aid and oxide on particle surface
Glass films in $\text{Al}_2\text{O}_3$	Mechanical	Impurities in the glass can affect its properties
Bismuth oxide in ZnO	Electrical	The IGF is the key to the operation of varistors
YAG in AlN	Thermal	$\text{Y}_2\text{O}_3$ added as sintering aid to allow lower cost production of substrates
Surface contamination	Chemical	Oxidation of SiC can passivate the surface
Clean GB in YBCO	Electrical	GB may not be superconducting; if very thin it can act as weak links

rapid deformation of the material. In other circumstances, the presence of the glass may be beneficial since it may assist in the branching and blunting of cracks by generally weakening grain boundaries.

- It is much easier to process ceramics in the presence of a liquid phase, in part for the same reason—the glass allows deformation at lower temperatures; diffusion is also faster through a glass. The glass thus allows the sample to be shaped and/or densified at lower temperatures.
- The composition of the IGF may vary across its width. In Figure 14.27, the rare-earth dopant has formed an La-rich monolayer at the glass/crystal interface.

It is well known that the presence of glass in GBs greatly enhances sintering, in part because transport of

matter along and across the intergranular regions is then even faster than when no glass is present. It is important to realize that the glass does not simply act as a catalyst, but also changes the character of the interfacial regions. The glass can dissolve the crystalline grain and reprecipitate it elsewhere. In particular, it tends to encourage faceting of the grains; the scale of this faceting may vary from nanometers to micrometers. After processing, the glass may remain as a thin layer in the interface during preparation of the polycrystalline compact as was initially demonstrated for  $\text{Si}_3\text{N}_4$ . The glass may also crystallize to form an intergranular crystalline layer or it may withdraw from the planar interfaces into three-grain and four-grain junctions (the dewetting process). Even though great care may be taken to ensure that no glass is present during processing, the glass may subsequently enter the interfacial region during processing or service of the component. In either case, the properties of the ceramic may be greatly influenced by the presence of any glass in the grain boundary; a dramatic example is the effect on mechanical properties (e.g., for  $\text{Si}_3\text{N}_4$  or  $\text{Al}_2\text{O}_3$ ), which also aids sintering, although other properties (e.g., the thermal conductivity for AlN) may be just as strongly affected.

Figure 14.28 illustrates another feature associated with glass in crystalline ceramics. The pairs of grains joining at these two boundaries are similarly oriented. Both of the interfaces contain dislocations, i.e., they were glass free after processing. The topology of the two interfaces is, however, clearly different. In Figure 14.28a the interface is wavy, while in Figure 14.28b it is flat. The difference can be explained by the processing history; the bicrystal in Figure 14.28b initially contained a layer of glass, while that in Figure 14.28a was kept as clean as possible during processing. So the difference in the topography is ascribed to the effect of the glass while it was present in

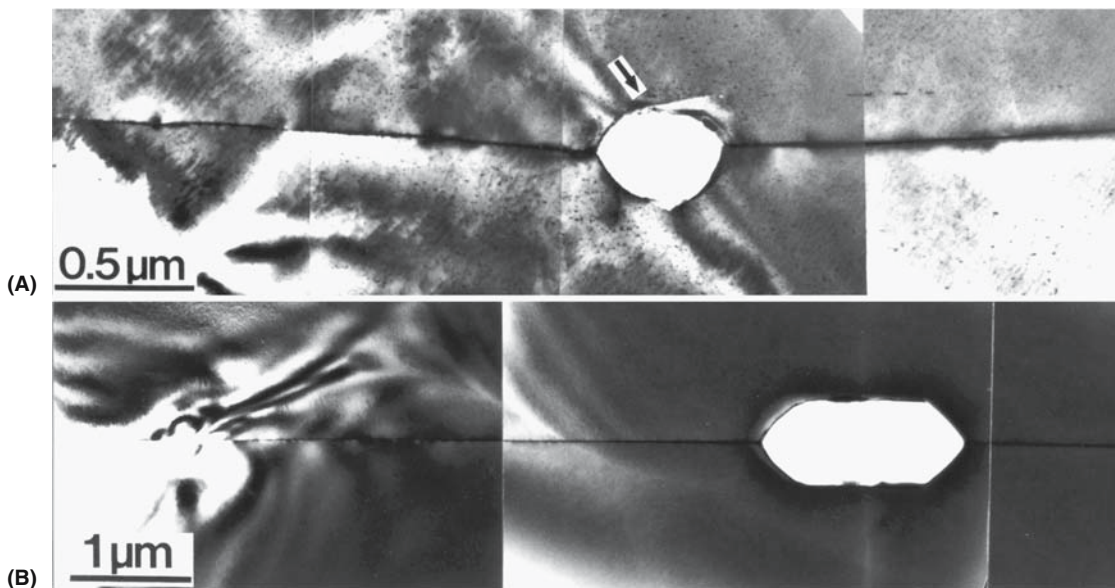


**FIGURE 14.28** The same GB in  $\text{Al}_2\text{O}_3$  processed with and without glass.

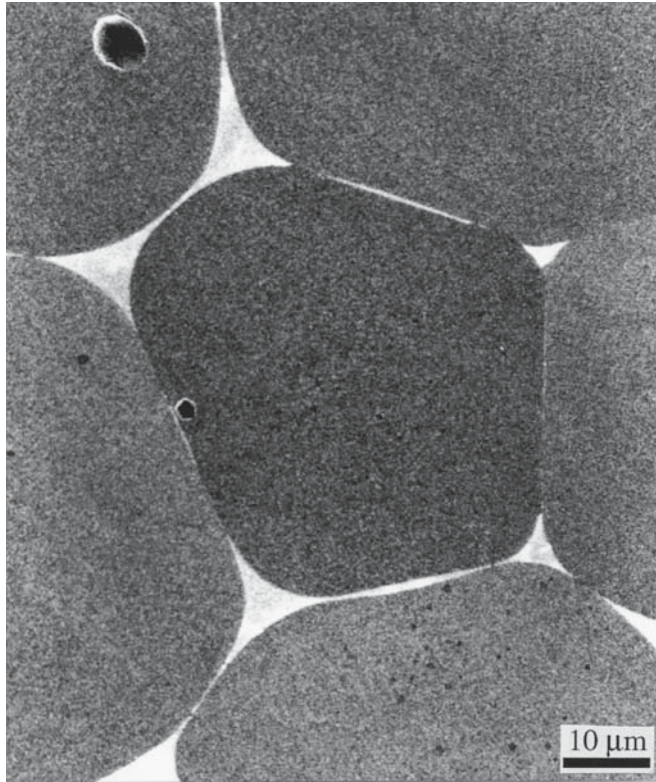


**FIGURE 14.29** SEM image of glass-infiltrated MgO showing glass located at the GB and at TJs, but even in a GB it need not be a uniform layer.

the interface. Clearly this effect can potentially be very important in understanding such GBs, but it presents a major difficulty; the key component required to explain the structure of the GB had already disappeared before the processed compact could be examined.

Water in silicate GBs can significantly change the mechanical properties of the GB. The GBs really are wet in the everyday sense! The crystal structure of the grains causes ordering in the water and thus changes the viscosity of the water.

The behavior and effects of water in GBs are important topics in geology. There has been much discussion on the thickness of intergranular glass films. There may be an equilibrium thickness for such films, as has been reported for  $\text{Si}_3\text{N}_4$ , but a more common situation is shown in Figure 14.29. This sample was a dense, small-grain, glass-free polycrystal that was intentionally infiltrated with monticellite glass. Here the width of the glass layer clearly varies from boundary to boundary and even along a particular boundary. Nearby boundaries can show a layer that is nearly uniformly  $2\mu\text{m}$  wide or that is apparently glass free at this magnification. This image illustrates an important factor that is often overlooked: most of the glass is contained in TJs and QJs. These junctions serve as “pipes” for transporting the glass. Very little is known of the

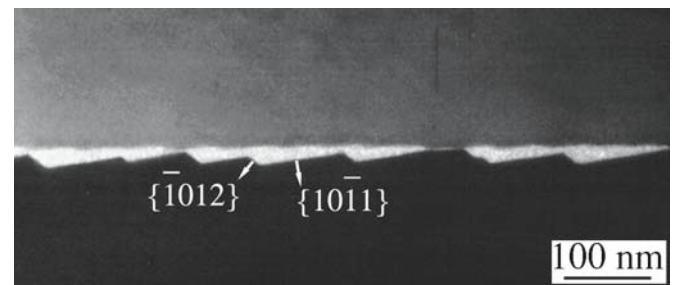
characteristics of TJs (they are not TEM friendly) or their role in determining mechanical properties.

Figure 14.30 shows a  $\Sigma = 13$  GB in alumina that was processed with an initial layer of anorthite glass that had a uniform thickness of  $\sim 100\text{nm}$ . The glass is still present in the interface after processing, but it varies in thickness along its length. Here the explanation for the thickness variations is clear: the two glass/crystal interfaces facet independently except in the regions where they appear to touch. The controlled preparation of such interfaces is not, in principle, limited to special boundaries, since any two such surfaces can be so joined and both the composition and the initial amount of glass can be predetermined and controlled.

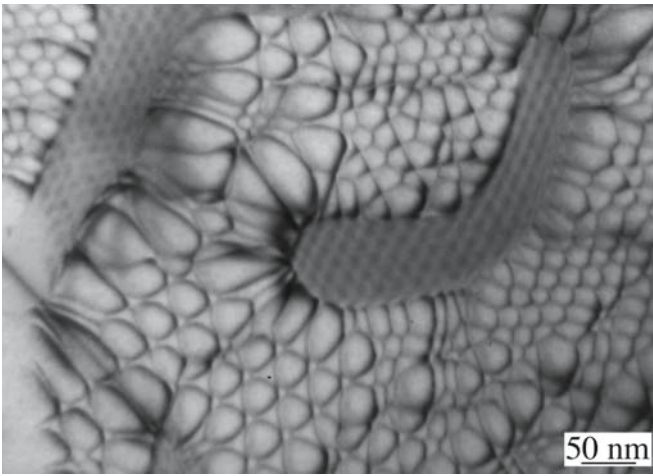
Dewetting of GBs has been observed in Si where the glass was the native oxide,  $\text{SiO}_x$  ( $x \sim 2$ ). Figure 14.31 shows TEM images of a  $\Sigma = 1$  (low angle)  $\langle 110 \rangle$  tilt boundary and a  $\Sigma = 5$  (001) twist boundary. In both cases abrupt changes in contrast can be seen where the glass has dewetted the interface to accumulate in pockets. The pockets actually facet parallel to  $\{001\}$  and  $\{111\}$  planes due to the crystallography of the Si. Thus, even the  $\Sigma = 5$  GB can achieve its low-energy structure, including the secondary dislocations, in the presence of a dewetting glass film.

Crystallizing intergranular glass layers after processing has been used to modify the mechanical properties of the resulting compact. The yttria-rich glass in polycrystalline  $\text{Si}_3\text{N}_4$  and monticellite glass in MgO can be crystallized after liquid-phase sintering to change the properties of the polycrystal.

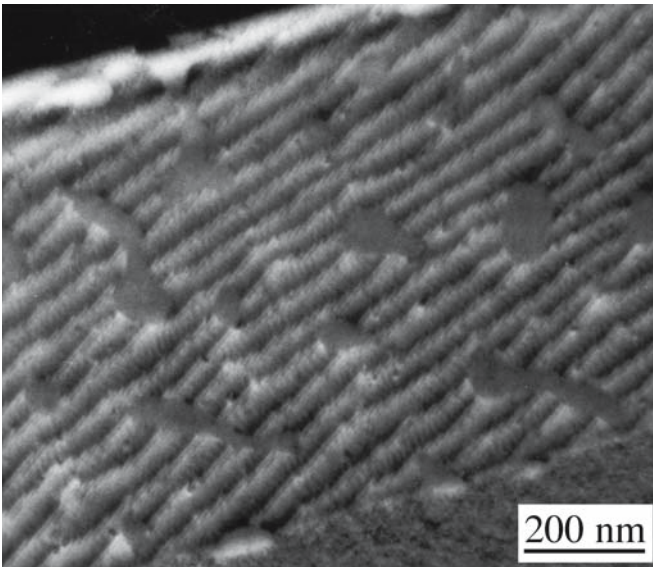
An important remaining question concerns how the presence of the second glass/crystal interface (in a GB) might affect the crystallization process. If topotactic crystallization nucleates at one glass/crystal interface, it is unlikely that the crystallizing glass will form a complex (high-energy) interface when it reaches the adjacent grain. Similarly, if crystallization nucleates at both glass/crystal interfaces, a complex grain boundary, possibly with residual glass, will form when the crystallized glass layers grow together.



**FIGURE 14.30** An IGF in  $\text{Al}_2\text{O}_3$  that was initially uniformly thick varying in thickness after heat treatment.



(A)



(B)

**FIGURE 14.31** Dewetting of IGFs in Si GBs: (a)  $\Sigma = 1$  {111}; (b)  $\Sigma = 5$  {001}.

### 14.9 TRIPLE JUNCTIONS AND GB GROOVES

We will not spend much time on TJs because not much is known about them. We can identify three different types of TJ.

1. One composition: Three-grain junctions
2. Two compositions: Two phase boundaries plus a GB
3. Three compositions: Three phase boundaries

Thus, for example, the groove formed when a GB emerges at a free surface is an example of a two-composition triple junction. Three TJs meet at a QJ. The pockets of second phase at TJs in Figure 14.32 could each be considered as sets of three two-composition TJs. Incidentally, looking at the surface will not give us an unambiguous picture of the dimensions.

A schematic diagram showing how GBs, TJs, and QJs change with changes in wetting behavior is shown in Figure 14.33. Wetting is clearly important when we process ceramics using a liquid phase. For the liquid phase to be effective in densification we want it to wet the grains, hence  $\phi = 0$ . But for optimum properties of the final ceramic we may not want the grains covered with a second phase. A good example is in AlN ceramics for electronic packaging. The second phase, which will almost always have a much lower thermal conductivity, should form isolated pockets at the TJs leaving a “clean” GB enabling maximum phonon transport.

A TJ can act like a capillary. The TJ in Figure 14.34 was covered with liquid glass at the processing temperature. When the sample was cooled, the liquid withdrew into the TJ like water escaping a bath (but the physics is different).

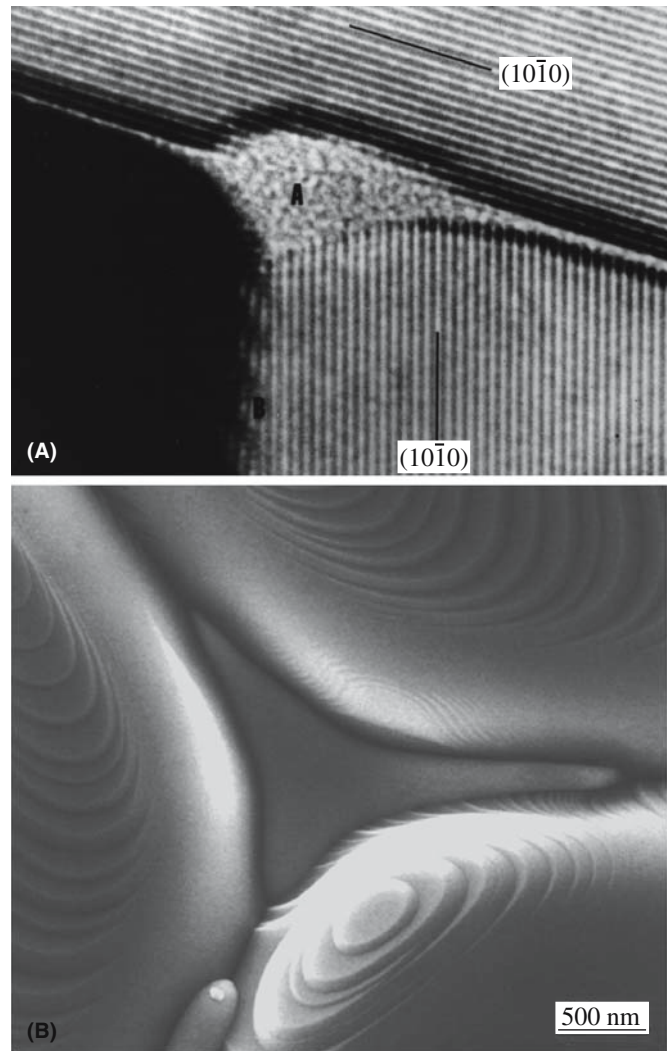


**FIGURE 14.32** Examples of TJs: (a)  $\text{Si}_3\text{N}_4$  using TEM; (b) MgO using SEM.

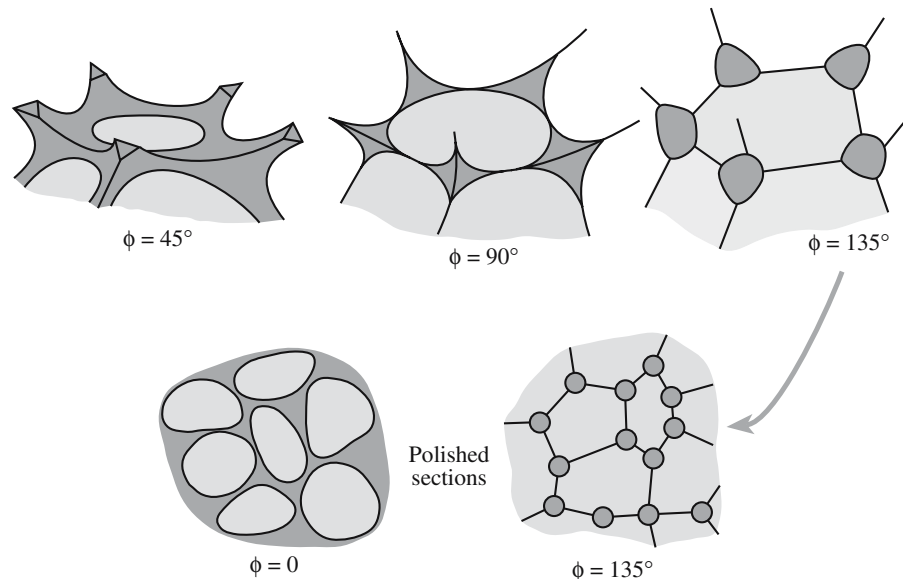


**FIGURE 14.33** Schematics showing the relationship between IGFs, TJs, and QJs in 3D as the wetting angle is changed. Lower: a reminder that we usually see sections of these structures.

## 14.10 CHARACTERIZING GBs

When studying a GB, we want to know the structure, chemistry, and bonding. How do we characterize a GB? What are the parameters we need? Just to understand the structure, we have to know all the crystallographic parameters, then the chemistry, and then the bonding. No single technique gives us all this information. No ceramic GB has been fully characterized, although we are getting close with a few.

Plane of boundary—Is the GB flat?

Axis of misorientation—The GB is an internal interface, so we need the orientations of both grains.

Atomic structure of boundary—The GB must be flat for HRTEM.

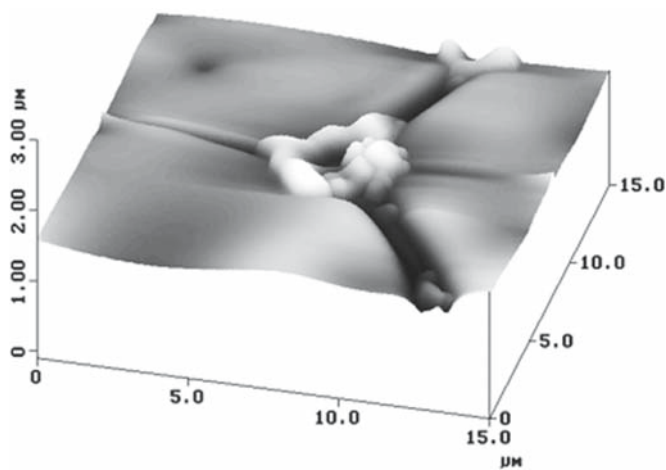


**FIGURE 14.34** Direct evidence for the capillary effect at a TJ; the glass recedes into the TJ on cooling.

Internal interfaces are fundamentally different from surfaces because of their inaccessibility. The key tool for studying GBs is the TEM. This should be obvious from the number of TEM images in this chapter! Although the material must usually be thinned prior to examination in the TEM, the area of the GB we do examine is unchanged.

TEM can be used to observe a periodic array of edge dislocations; we use Burgers circuit to characterize the dislocations

We can probe a GB by STM only where it intersects the surface. Atomic force microscopy, however, (AFM) is a key tool for characterizing GB grooves

*The specimen preparation problem for TEM:* GBs in ceramics must be considered in terms of both their structure and chemistry (even in so-called pure materials). Just as the wetting behavior of a surface may be altered by the doping of the surface layer, so it is important to identify and characterize the segregation of impurities and additives to GBs in these materials. The problem here is 2-fold: the features of the GB (its misorientation and plane) must be identified and the distribution of “foreign” elements must then be accurately measured. The last part of this process is actually even more difficult than you might expect. The added complexity arises from the methods that are, at present, routinely used to prepare samples of ceramic materials for examination in the TEM.

The TEM specimen is usually thinned by ion-milling; crushing will fracture the sample along GBs. This thinning process has been shown to result in cross-contamination of the specimen and in the formation of a groove at the interface. The degree of contamination depends on a large number of factors:

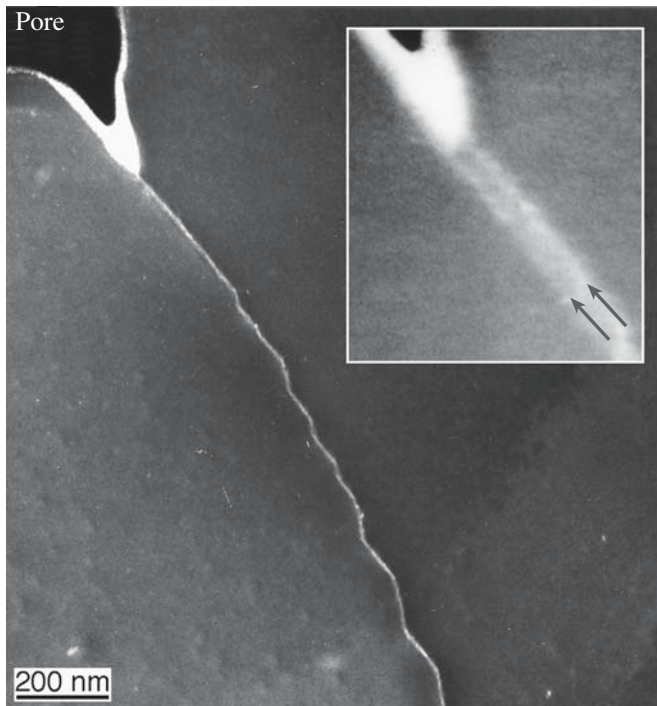


**FIGURE 14.35** A cautionary tale: the “glass” in the faceted GB is actually material deposited in surface grooves during sample preparation.

- The type of oil used in the diffusion pump of the ion-miller (old ion-millers may use a silicone-based diffusion pump oil since it is less expensive and more resistant to cracking than are Si-free oils).
- The cleanliness of the system used to carbon coat the thinned TEM specimen.
- The ion-thinning process also preferentially removes the lighter atoms and may deposit what it removes somewhere else on the sample.
- Ion thinning can implant Ar into loose, or open, structures (like GBs).
- Ion thinning may thus both preferentially thin the GB (forming a groove) and then deposit material in that groove. (Figure 14.35 shows the problem.)

It is always best to use bicrystals for model experiments to relate the chemical profile of an interface to its structure since we can then know the initial composition of the GB, but these are not “real” materials.

The principal techniques are

- The Fresnel-fringe technique
- The diffuse-scattering technique
- Direct lattice-fringe imaging where the geometry of the interface is suitable

The diffuse scattering technique suggests amorphous-film thicknesses that are 50–100% larger than are found by high-resolution EM (HREM), i.e., at least part of the image obtained from diffusely scattered electrons must be

due to factors other than the presence of a thin amorphous film. It is important to use a combination of techniques to characterize, as fully as possible, any given interface. For example, diffuse scattering is very dependent on the specimen preparation techniques. The reasons for using these techniques can be appreciated by noting that the amorphous layer, which may be present at the interface, may be only 1 nm wide. The complexity of image interpretation when examining thin (1–>5 nm wide) GB films makes computer analysis and simulation necessary. We can use image simulation programs to simulate the formation of Fresnel fringes, taking into account the possibility of GB grooving at both surfaces.

## 14.11 GBs IN THIN FILMS

Why are we interested in this topic? Ceramic thin films are becoming increasingly important in the electronics industry for their novel magnetic and electrical properties. Often these films are neither amorphous nor single crystal, so GBs become relevant. There will be TJs in the film and at the substrate/film interface (even if the substrate is amorphous). The TJ can form a pit (a 3D groove) at the surface, but it will generally not groove at the substrate.

Figure 14.36 is a dark-field TEM image from recrystallized anorthite glass on sapphire. The substrate appears dark and the anorthite grains have faceted edges.

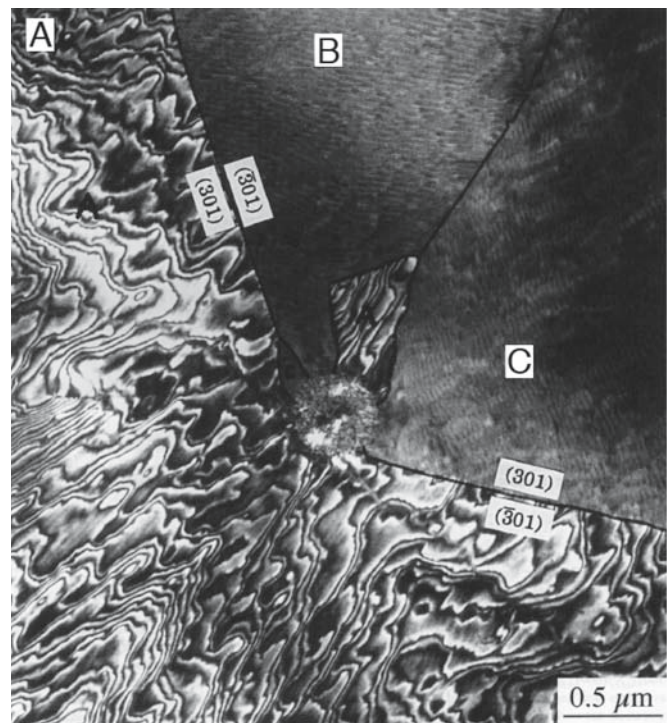


**FIGURE 14.36** Example of GBs in thin films of anorthite on  $\text{Al}_2\text{O}_3$ ; the three grains correspond to three epitaxial orientations, but only one shows the misfit dislocations in this TEM image.

The facets often meet at 60° or 120° angles. The three orientation variants are shown as A–C. Two TJs between all three variants can be seen in the image. Variant A contains irregular contrast associated with the interfacial dislocation network; variants B and C show moiré fringes.

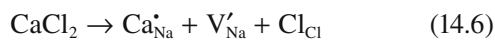
## 14.12 SPACE CHARGE AND CHARGED BOUNDARIES

We introduce this topic now because it shows the fundamental relationship between point defects and interfaces. The concept of a space charge is special for ceramics. Simply put, it is possible for an excess charge of one sign to be present at the interface. This excess charge must be balanced by a space charge further away from the boundary. There is not much experimental data, but the concept is widely accepted.

Consider NaCl: ions on either sublattice can, in principle, move to a new site on the GB leaving a vacancy in the lattice.



In general, the energy required to form these point defects at the GB is not the same as it is in the bulk and differs for the two ions. We therefore get more of one than the other at the grain boundary. Overall, the crystal is neutral, hence there must be a space charge in the bulk. Now add CaCl<sub>2</sub> to the NaCl crystal. The impurities (or dopants) give charged point defects.



We are adding the positively charged Ca<sup>2+</sup> ion and are thus increasing the concentration of vacancies on the Na sites. We know that



So, adding CaCl<sub>2</sub> to the bulk decreases [V<sub>Cl</sub><sup>•</sup>] in the bulk (because it increases [V'\_{Na}]). Since we have increased [V'\_{Na}] in the bulk, [Na<sub>GB</sub><sup>•</sup>] must decrease in the GB, which implies that [Cl'\_{GB}] increases in the GB. Hence the GB potential is negative. There is a complication: what about Ca<sub>Na</sub><sup>•</sup>? What if it all goes to the GB? The radii of the Ca<sup>2+</sup> and Na<sup>+</sup> ions are about the same (~0.1 nm). We do not know the radius of the Ca ion on the Na site. We have also not considered the possibility of forming a defect complex such as (Ca<sub>Na</sub><sup>•</sup>, V'\_{Na}); the binding energy is quite large, ~0.4 eV. The idea of the GB space charge is therefore important, but far from simple, and there is not much experimental data.

## 14.13 MODELING

The extensive analysis of the structure of GBs in ceramic oxides using computer modeling does not appear yet to explain the experimental observations. One limitation of the modeling approach is that the GB plane is fixed in the calculation. Furthermore, computer modeling of asymmetric interfaces is not routine—constructing the unit cell for asymmetric GBs is difficult. Most of this computer modeling has been directed at understanding the structure of GBs in materials with a rocksalt structure. In these materials (primarily NiO and MgO), the oxygen-ion sublattice is in an fcc arrangement whereas the cations are located at the octahedral sites. The situation is more complex for most other oxides when different interstices are occupied; as you know, in spinel two-thirds of the cations occupy octahedral interstices while one-third occupies tetrahedral interstices.

We cannot assume that all the ions have found their “ideal” sites in sintered material, e.g., some Al<sup>3+</sup> ions in MgAl<sub>2</sub>O<sub>4</sub> may be on tetrahedral sites. The structure predicted by computer modeling for the {112} lateral twin interface in NiO contains a rigid-body translation. Such a translation is not observed experimentally for the same type of interface in spinel, which has the same oxygen sublattice. It may be that the reason for this difference is that the translation-free configuration is what is present on a migrating GB and this becomes “frozen in” when the sample is cooled. The structure predicted by minimum energy calculations is a stationary structure.

The disagreement between experiment and modeling may be also due to the difficulty in preparing ideal clean interfaces in ceramic materials. For example, the Σ = 5 GB in NiO can be stabilized by adding Schottky defects to the interface, i.e., by decreasing the density at the GB while keeping it “pure.” Experimental observations do show that the density at interfaces is generally lower than that of the bulk material.

Most programs use a cell that repeats the structure of the GB and, hence, most calculations have been carried out for low-Σ GBs.

## 14.14 SOME PROPERTIES

GBs are everywhere in ceramics. The formation of GBs will be discussed in Chapter 24 since this is the initial product of the sintering process. The movement of GBs is the necessary process allowing grain growth to occur and will also be discussed there. GBs influence the behavior of polycrystalline ceramics—both bulk materials and thin films. We will discuss their properties extensively in later chapters. Here we just list a few examples so you can see their importance.

Example 1: GBs are probably the most important defect in ceramic superconductors. They can dramatically

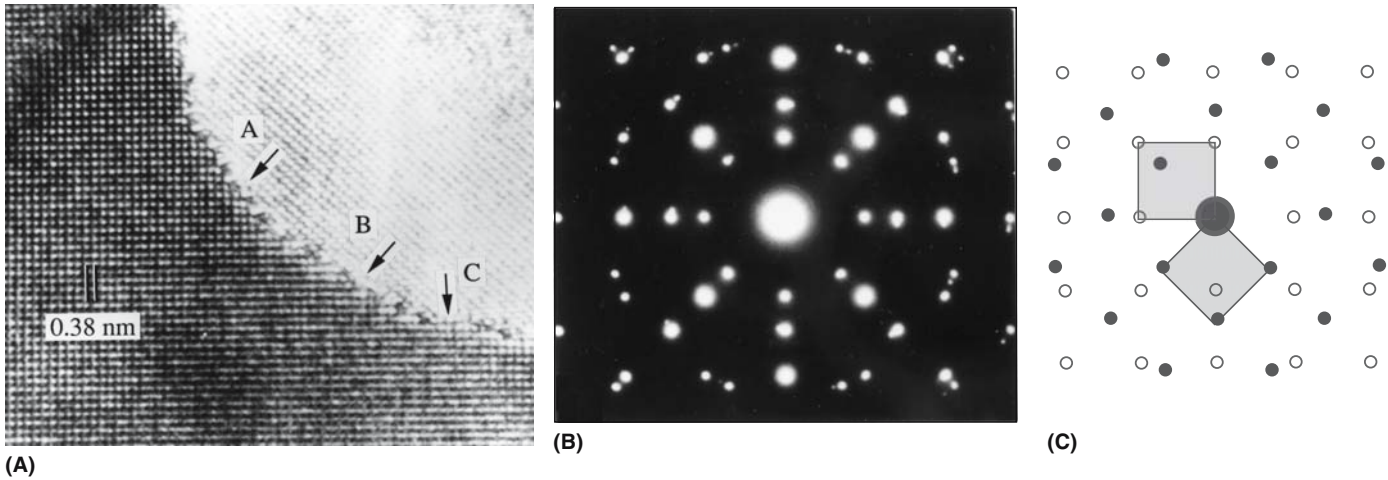


FIGURE 14.37 HRTEM image of the 45° GB in YBCO and the diffraction pattern.

reduce critical currents ( $J_c$ ). The idea is that the GB acts as if it is a second phase. This sheet is not a superconductor—it may act like a sheet of insulator inside the superconductor. If the GB is very thin then it is possible to use its weak-link nature to fabricate a Josephson junction. Figure 14.37 is an HRTEM image of a near  $\Sigma = 29$  GB in a YBCO thin film. The GB is narrow, abrupt, and faceted. We will revisit this topic in Chapter 30.

Example 2: GBs in AlN can reduce the thermal conductivity if they are not clean. Because AlN is difficult to sinter to high density without the use of a liquid phase (the bonding is mainly covalent), the GBs often contain a second phase, which always has a lower thermal conductivity (Chapter 34). Ytria may be added to react with oxide in the GBs to form YAG at the triple junctions: a GB-dewetting process.

Example 3: GBs in ZnO are processed intentionally to include a glass film. This film allows the ceramic to be used as a varistor (voltage-dependent resistor), a device that protects circuits from high-voltage spikes (Chapter 30). Figure 14.38 illustrates an IGF of varying thickness in ZnO and how this film controls the resistance.

Example 4: GBs in  $\text{Si}_3\text{N}_4$  invariably contain glass films as shown earlier. At high temperatures they can lose their mechanical strength when the films soften (Chapter 18).

Example 5: GBs in magnetic ferrites affect the initial permeability,  $\mu$ . The permeability of Mn-Zn ferrite increases from about  $0.8 \times 10^{-3}$  up to  $3.5 \times 10^{-3}$  when the grain size is increased from  $5 \mu\text{m}$  to  $15 \mu\text{m}$  (Chapter 33). Although porosity has a role, it has been determined that grain size is more important.

Example 6: GBs affect the scattering of light in transparent materials. Light scattering is greatest when the grain size is close to the wavelength. In addition, IGFs produce a change in refractive index as light passes through a material (Chapter 32).

In metals, GBs control mechanical properties when the grain size is small as seen from the Hall–Petch equation

$$\sigma_y = \sigma_0 + \frac{B}{d^{1/2}} \quad (14.8)$$

The yield strength ( $\sigma_y$ ) is expressed in terms of the yield stress,  $\sigma_0$  ( $\sigma_0$  is related to the intrinsic stress,  $\sigma_i$ , resisting dislocation motion) and the grain size,  $d$ . When this relationship was deduced, it applied to a situation in which the grains were deformed by plastic deformation and the GBs acted as barriers to dislocation motion. This model is unlikely to be valid in general for ceramics since deformation by dislocation glide is not common. However, the relationship between  $d$  and  $\sigma_y$  does hold as we saw for polycrystalline MgO in Figure 1.2.

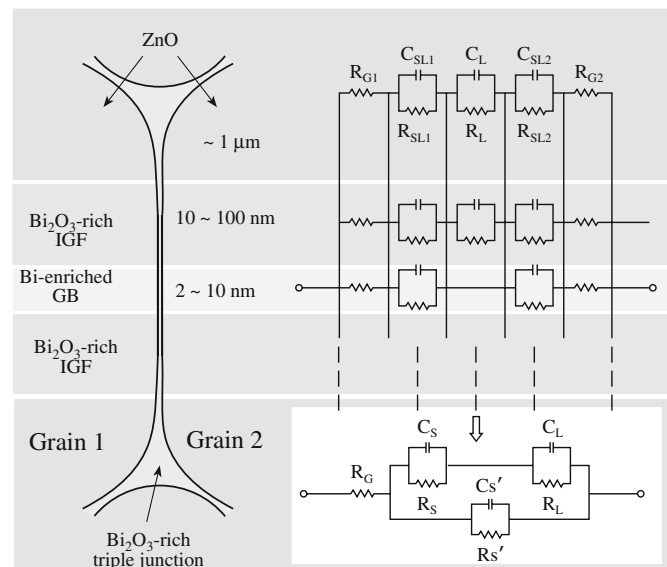


FIGURE 14.38 Modeling IGFs in ZnO varistor materials.

## CHAPTER SUMMARY

GBs in ceramic materials are important in almost all applications of these materials since ceramics are usually polycrystalline. GBs have a thickness—we can think of them as thin films even if they are structured. This means that a polycrystalline material is really a composite one. An added difficulty is that essentially every GB “film” is different, but we can think of an *average* GB, which is especially good if there actually is an amorphous film (IGF) at the interface. The most important point to remember is the relationship between GB energy and GB (interface) tension, which includes the idea that there is a pressure difference across a curved GB just as there is across a curved surface. You should be able to define the words twist, tilt, mixed, and twin and to understand the concept of  $\Sigma$  (and  $\Gamma$ ), how it relates to structure, and why it can be related to GB energy. Triple junctions and the space charge at GBs are very important, but we know little about them. There are two special features for ceramics: the space charge and IGFs. IGFs are special for ceramics because glass is easily formed and maintained, especially when the ceramic contains at least small concentrations of Si.

### PEOPLE IN HISTORY

Bollmann, Walter was a pioneer in explaining the O-lattice concept.

Friedel, G. and Friedel J. were early contributors to the development of the CSL.

Matthews, John was best known for his work on misfit, epilayer growth, and MgO smoke.

Mullins, William W. explained and predicted observations on GB grooving. He died in 2002.

### GENERAL REFERENCES

Grain boundaries have been extensively reviewed in several recent books. These texts cover all crystalline materials, but you will still need to go to the original papers to learn more about GBs in ceramics.

Bollman, W. (1970) *Crystal Defects and Crystalline Interfaces*, Springer-Verlag, New York. The original book giving the analysis of  $\Sigma$ , O lattice, etc.

Howe, J.M. (1997) *Interfaces in Materials: Atomic Structure, Thermodynamics and Kinetics of Solid/Vapor, Solid/Liquid and Solid/Solid Interfaces*, John Wiley & Sons, New York. A very readable book with a practical emphasis.

Hull, D. and Bacon, D.J. (2001) *Introduction to Dislocations*, 3rd edition, Butterworth-Heinemann, Philadelphia, A review of the basics.

Kelly, A., Groves, G.W., and Kidd, P. (2000) *Crystallography and Crystal Defects*, John Wiley & Sons, New York. Not broad or up-to-date but an excellent basic text.

Read, W.T. and Shockley, W. (1950) “Dislocation models of crystal grain boundaries,” *Phys. Rev.* **78**(3), 275. A classic readable paper with great diagrams.

Smith, D.A. and Pond, R.C. (1976) “Bollman’s O-lattice theory: a geometrical approach to interface structure,” *Inter. Met. Rev.* **205**, 61. Very readable discussion of the background to the GBs.

Stokes, R.J. and Evans, D.F. (1997) *Fundamentals of Interfacial Engineering*, John Wiley & Sons, New York. Bob Stokes retired from Honeywell and joined the University of Minnesota part time.

Sutton, A. and Balluffi, R. (1996) *Interfaces in Crystalline Materials*, Oxford University Press, Oxford, UK.

Wolf, D. and Yip, S. (Eds.) (1992) *Materials Interfaces: Atomic-Level Structure and Properties*, Chapman & Hall, London.

### SPECIFIC REFERENCES

Amelinckx, S. (1958) “Dislocation patterns in potassium chloride,” *Acta Met.* **6**, 34. Seeing GBs in KCl by decoration.

Chaudhari, P. and Matthews, J.W. (1971) “Coincidence twist boundaries between crystalline smoke particles,” *J. Appl. Phys.* **42**, 3063. Original description of the MgO smoke experiment for GBs

Zhu, Y. and Granick, S. (2001) “Viscosity of interfacial water,” *Phys. Rev. Lett.* **87**(9), 096104. The idea is that the viscosity of water can be very different if it is constrained to be a film in a silicate grain boundary.

### EXERCISES

- 14.1 Using the idea of capillarity and relating it to a triple junction, what happens as the temperature increases (so that viscosity decreases)?
- 14.2 Consider a 1-cm cube of a 100% dense ceramic that contains 5% glass that can wet the crystal grains. If the grain size changes from 100 nm to 10 mm due to heat treatment, how does the distribution of the glass change? Be careful to summarize your assumptions and list as many variables as you can.

- 14.3 Consider two small-angle ( $2^\circ$ ) tilt grain boundaries in MgO, both having a [001] tilt axis. For one the boundary plane is nearly (100) while for the other it is (110). Discuss the structure of these two grain boundaries.
- 14.4 The structure of the spinel,  $\text{MgAl}_2\text{O}_4$ , projected onto the (110) plane is shown in Figure 7.1b. Spinel twins on {111} planes. Draw all the different allowed structures for the coherent (IT) plane and discuss which of them is most likely to occur giving clear reasons. Consider how your analysis might change if the spinel was not equimolar.
- 14.5 If the surface energy for (001) MgO is  $1\text{J/m}^2$  what is that in electron volts per oxygen ion on the surface. How does this number compare to the formation energy of the Schottky defect? How would this number be different if the material were NaCl instead of MgO?
- 14.6 Dislocations in a tilt boundary on the (011) plane in silicon lie 200nm apart. What is the misorientation of the two grains. Would the etch-pit method be a good way to examine this boundary? Explain your answer.
- 14.7 (a) For the TJ shown in Figure 14.34 derive a relationship between  $\gamma_{\text{GB}}$ ,  $\gamma_{\text{SL}}$ , and the dihedral angle,  $\phi$ , which is the angle subtended by the liquid. (b) Assuming that  $\gamma_{\text{SL}}$  is  $700\text{mJ/m}^2$ , determine  $\gamma_{\text{GB}}$ .
- 14.8 Construct a model for a  $\Sigma = 7$  twin boundary in sapphire that is also a tilt boundary with a [0001] rotation axis.
- 14.9 Consider what might happen to the grain boundary charge when MgO is added to  $\text{Al}_2\text{O}_3$ .
- 14.10 A tilt boundary in olivine lies on the (100) plane with a [001] rotation axis. The dislocations are all the same Burgers vector and are 100nm apart. What is the rotation angle?